In presenting the dissertation as a partial fulfillment of the requirements for an advanced degree from the Georgia Institute of Technology, I agree that the Library of the Institute shall make it available for inspection and circulation in accordance with its regulations governing materials of this type. I agree that permission to copy from, or to publish from, this dissertation may be granted by the professor under whose direction it was written, or, in his absence, by the Dean of the Graduate Division when such copying or publication is solely for scholarly purposes and does not involve potential financial gain. It is understood that any copying from, or publication of, this dissertation which involves potential financial gain will not be allowed without written permission.

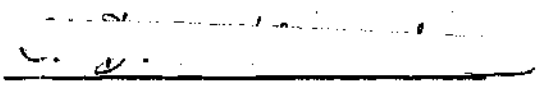

7/25/68

CHARACTERISTICS OF A VISCOUS FLOW COMPRESSOR

A THESIS

Presented to

The Faculty of the Graduate Division

by

Snit Dusadeenoad

In Partial Fulfillment

of the Requirements for the Degree

Master of Science in the

School of Mechanical Engineering

Georgia Institute of Technology

September, 1970

CHARACTERISTICS OF A VISCOUS FLOW COMPRESSOR

Approved:

Chairman

Date approved by Chairman: 10-16-70

ACKNOWLEDGMENTS

Much gratitude is due to Dr. G. T. Colwell, my advisor, for his valuable help and guidance, in obtaining the data and editing the several drafts of this thesis.

I would also like to thank members of my committee, Dr. Thomas W. Jackson, Dr. S. V. Shelton, Dr. M. R. Carstens, for their interest, careful reading and suggestions.

TABLE OF CONTENTS

LIST OF TABLES

LIST OF FIGURES

LIST OF FIGURES (Continued)

NOMENCLATURE

A_c	=	cross sectional area (ft^2)
A_w	=	the drag area (ft^2)
C_p	=	specific heat of fluid at constant pressure (btu/lbm-^oR)
d	=	hydraulic diameter. (ft)
f	=	friction factor for laminar or turbulent flow
g_c	=	gravitational constant (32.17 lbm-ft/lbf-sec^2)
g	=	acceleration of gravity (ft/sec^2)
H	=	height of rotor slot (ft)
h	=	specific enthalpy (btu/lbm)
J	=	heat equivalent of work (778 ft-lbf/Btu)
$\dot{M}$	=	mass flow rate through passage (lbm/sec)
n	=	unit vector
p_o	=	ambient pressure (lbf/ft^2)
p_1	=	pressure at the entrance of volume element (lbf/ft^2)
p_2	=	pressure at the exit of volume element (lbf/ft^2)
Q	=	heat transfer from fluid to casing (btu/sec)
R	=	gas constant (ft-lbf/lbm-^oR)
R_c	=	number of rotor slots
Re	=	Reynold's number of a specific volume element base on the hydraulic radius
T_o	=	Ambient temperature (^oR)
T_1	=	Temperature at the entrance of volume element (^oR)
T_2	=	Temperature at the exit of volume element (^oR)

T_3 = Laminar Flow Element Temperature ($^{\circ}R$)

u = Absolute rotor velocity at the mean radius of the rotor slot (ft/sec)

v = the control volume element

V = absolute fluid velocity through the rotor slot (ft/sec)

$V_{c.v.}$ = absolute velocity of the control volume (ft/sec)

$V_{f/r}$ = velocity of fluid relative to the rotor slot at the mean radius of the slot (ft/sec)

V_1 = absolute velocity at the entrance of a volume element (ft/sec)

V_2 = absolute velocity at the exit of a volume element (ft/sec)

W = width of rotor slot (ft)

$\dot{W}$ = the rate of work of the rotor on the fluid (ft-lbf/sec)

ΔZ = Length of volume element (ft)

Z = distance from reference elevation (ft)

ρ_1 = Density of the fluid at the entrance of the volume element (lbm/ft^3)

ρ_2 = Density of the fluid at the exit of the volume element (lbm/ft^3)

μ = absolute fluid viscosity at a temperature T(lbm/sec-ft)

μ_o = absolute fluid viscosity at a temperature of $70^{\circ}F$ (lbm/sec-ft)

τ_o = shear stress (lbf/ft^2)

η = adiabatic compression efficiency (%)

SUMMARY

A circumferential flow compressor with a seven inch titanium rotor, tesla blading, and graphite seals was studied experimentally and theoretically. Originally it was planned to operate the compressor between 15,000 RPM and 70,000 RPM. However, due to limited drive power and seal problems the unit was operated at a maximum rotational speed of 42,000 RPM. (~640 feet per second rim speed)

Pressures and temperatures versus flow rates were experimentally and theoretically determined. It was found that heat transfer greatly affected pressure rise at low flow rate for each rotor speed. A digital computer was used to simultaneously solve the continuity equation, momentum equation, energy equation, and equation of state. Geometry effects were studied in only a theoretical way. In addition the adiabatic compression efficiency was studied. The highest adiabatic compression efficiency was obtained at 24,000 RPM. Velocity and pressure along the flow arc were studied theoretically, as was the effect of geometry.

CHAPTER I

LITERATURE SURVEY

There are many papers which deal with developing and fully developed laminar and turbulent flows between flat plates with and without heat transfer. However, no reference has been located which treats the circumferential flow in a disk compressor with both circumferential entrance and exhaust, which is the system under consideration here.

The first six papers listed in the references are of general interest. For instance, the book by Shapiro (1) was used to design the intake nozzle while the book by Timoshenko (6) was used to determine stresses in the rotor.

Dorfman (7) studied several cases of flow near a rotating disk. Wall shears predicted in his book are remarkably close to wall shears measured during the present test program. Also the boundary layer thicknesses as computed from Dorfman's equations are of considerable value.

References (8 and 9) are interesting because they consider the effect of curvature on the compression process as well as studying boundary layer build up. It should be noted that these references are for laminar flow while the present studies concern turbulent flow.

Traviss (10) wrote the computer code which was used in predicting the theoretical results presented in this thesis. His analysis assumes that the flow is one dimensional and adiabatic. Thus the effects of curvature have not been included in the theory.

CHAPTER II

EXPERIMENTAL APPARATUS

All the experimental evaluations were obtained running a titanium wheel with graphite seals. The titanium wheel and a sectional view of the rotor assembly are shown in Figures 2-1 and 2-2 respectively.

2-1. Measurements

Figure 2-3 shows the experimental apparatus. A schematic of the peripheral compressor is shown in Fig. 2-4. The ambient conditions (P_o and T_o) were measured using a mercury barometer and thermometer. The absolute pressure and temperature (P_2 and T_2) at the compressor exit were determined by using a mercury manometer and a thermocouple. The angular velocity of the rotor was measured with an electric counter and a magnetic pickup. Volumetic flow rate at the exit was calculated from the pressure drop across a laminar flow element (Meriam, model 50 MCZ-ZP). The volumetic flow rate was then referred to standard temperature and pressure by means of the Meriam temperature-correction curve as shown in Appendix C-1. The mass flow or volumetic flow rate was regulated by a gate valve in the exit line. The temperature at compressor inlet (T_1) and outlet (T_3) were also measured with thermocouples.

There are two methods to measure compressor characteristic curves: first, the drive turbine flow and test compressor back pressure can be adjusted so that a constant speed curve is obtained; second, the compressor valve setting can be kept constant while varying drive turbine

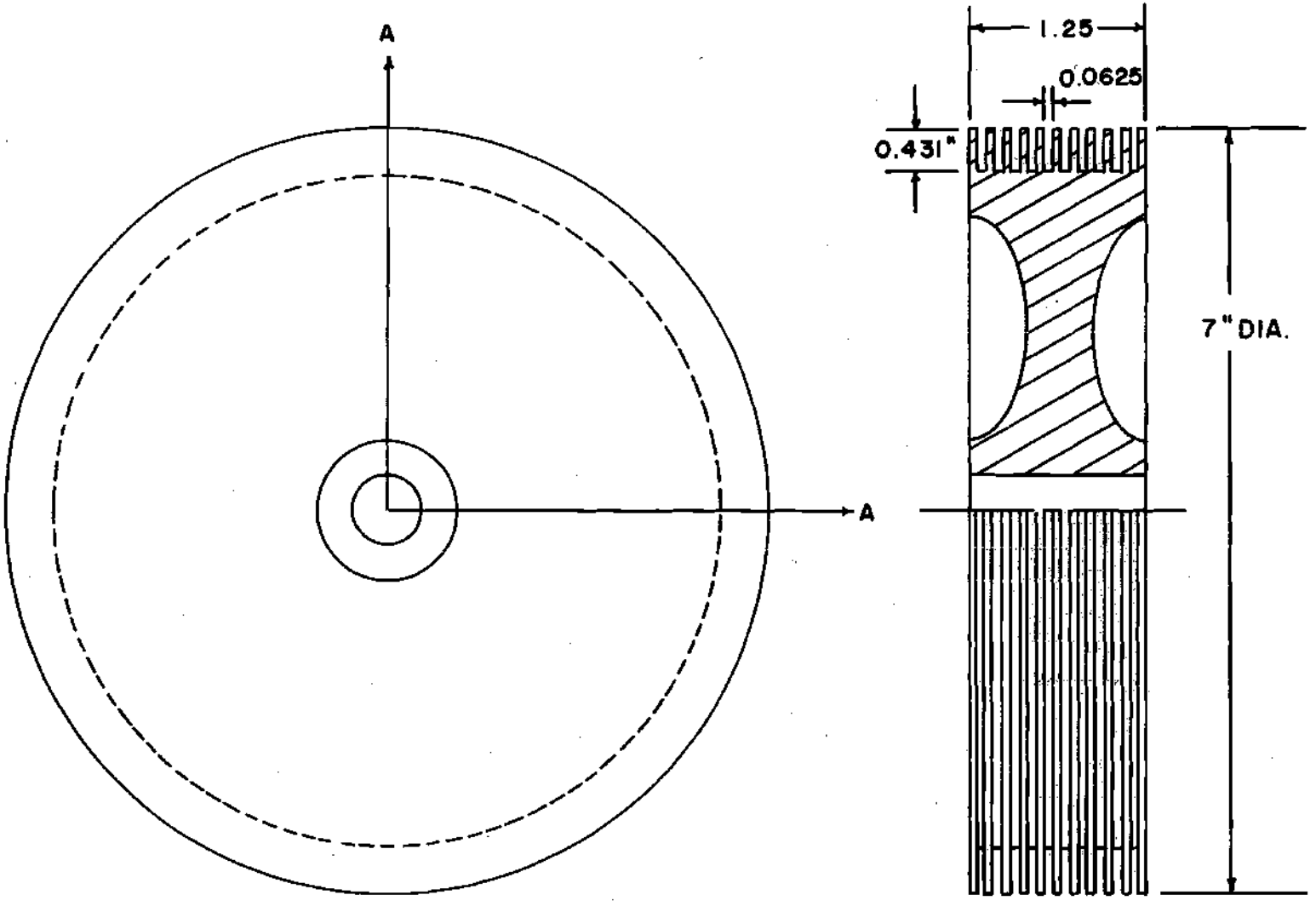

Figure 2-1. Titanium Wheel

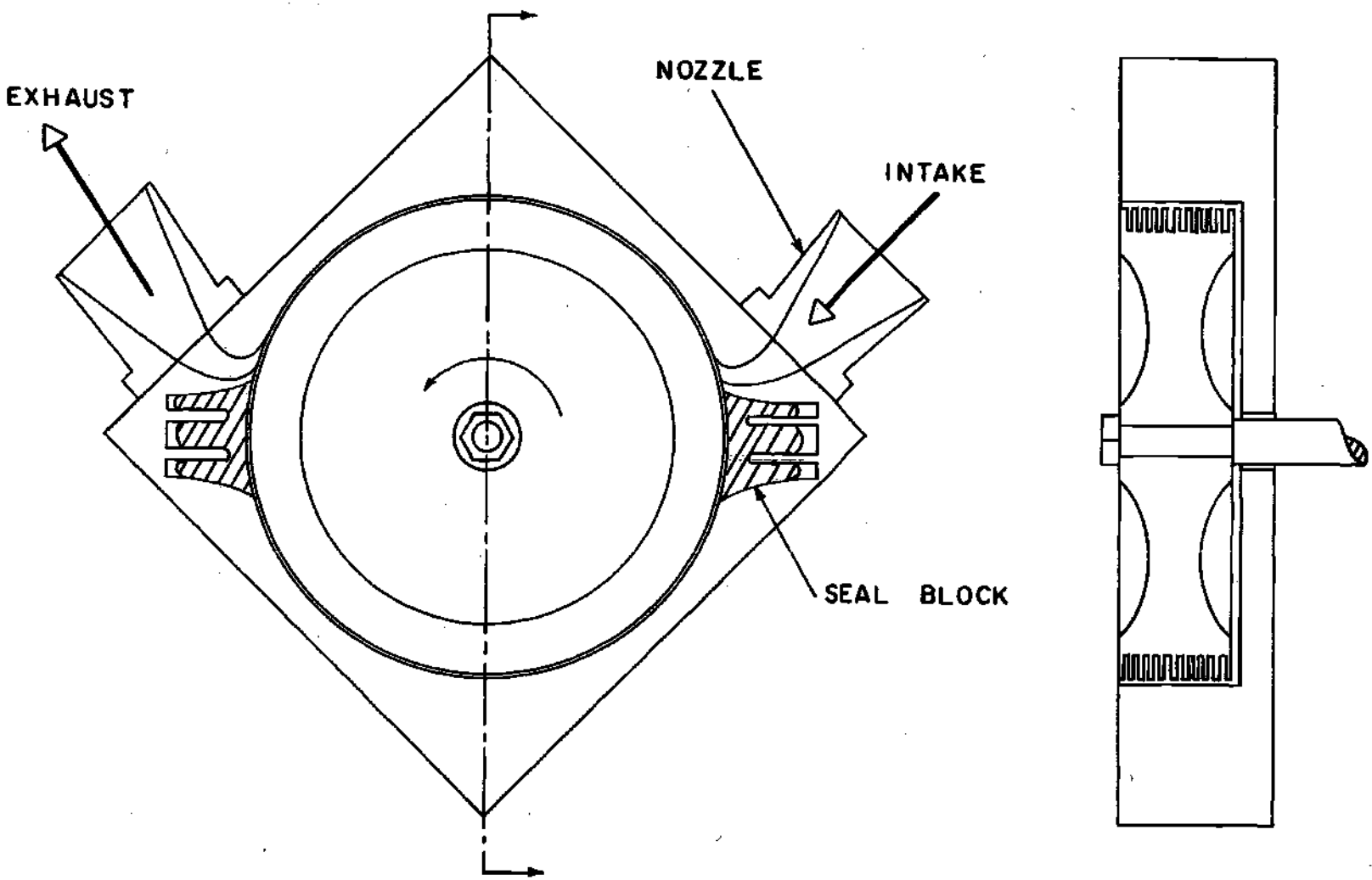

Figure 2-2. Sectioned View of Rotor Assembly

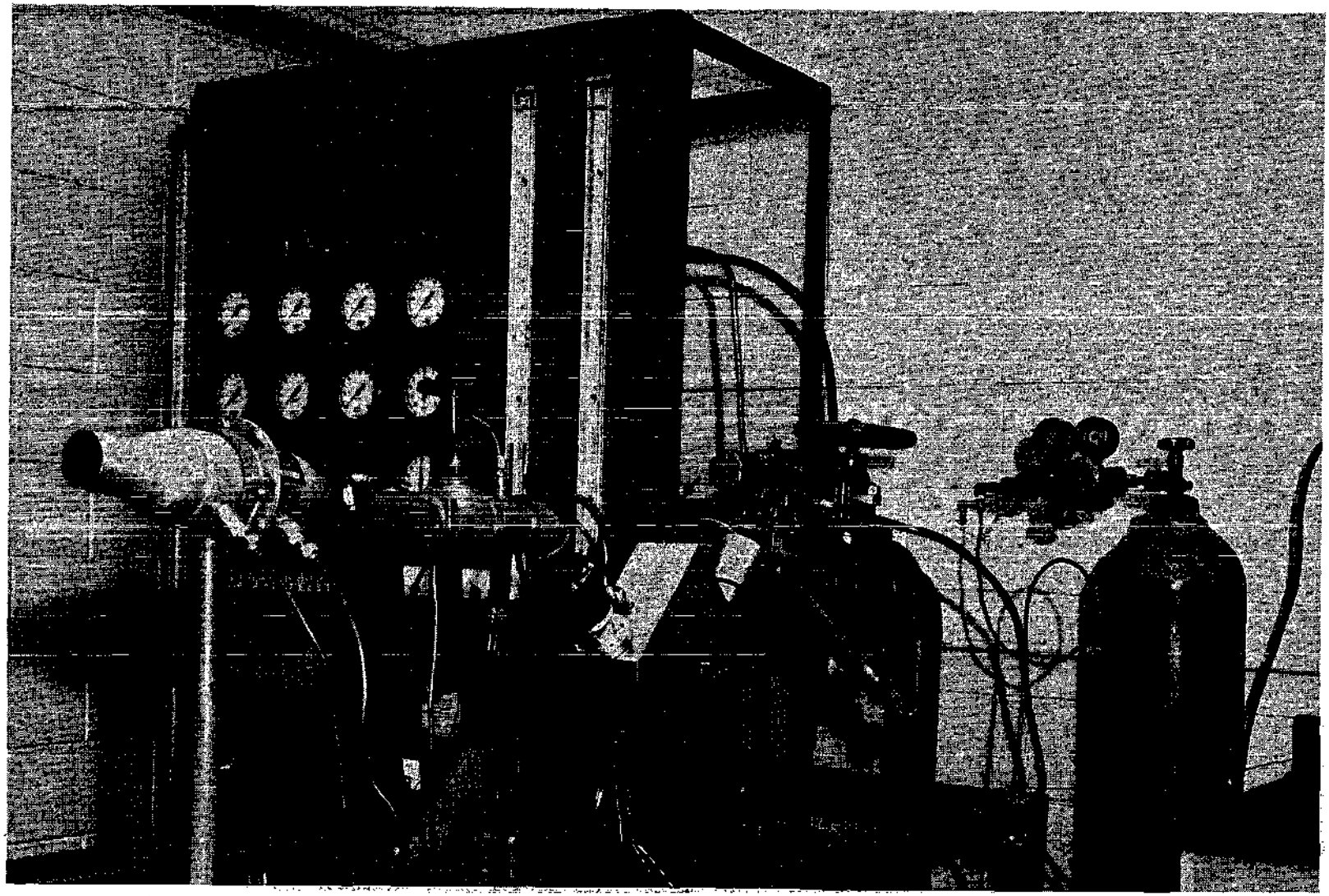

Figure 2-3. Experimental Apparatus

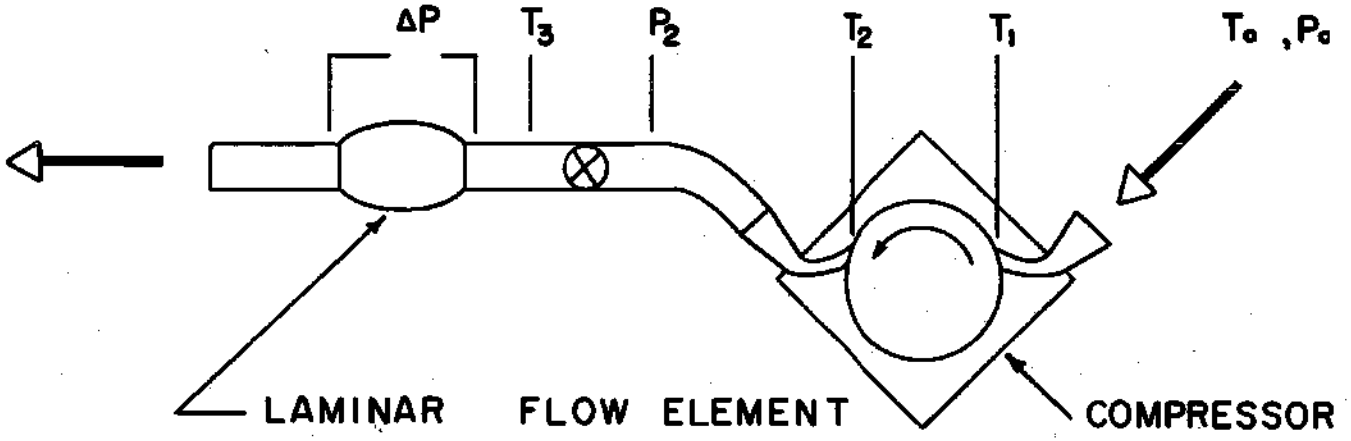

Figure 2-4. Schematic of Equipment

speed and thus determining performance for various constant system resistances. Using both methods, the temperature rise around the circumference and the temperature and pressure at the exit were recorded for each flow rate setting. The data are shown in the Appendix B.

2-2. Data Reduction

The experimental data were then used to calculate the pressure rise, the volumetic flow rate (SCFM) and the angular rotor speed (RPM). Pressure drops across a laminar flow element were used to compute volumetic flow rates through the machine. Flow rates were corrected for temperature variation using the information in Appendix C-1. Actual flow rates were then found from the information in Appendix C-2.

After reducing the data, performance curves of pressure rise versus volume flow rate and exit temperature versus flow rate at constant rotor speed were generated. Typical performance curves presented in Chapter IV.

CHAPTER III

DEVELOPMENT OF THEORETICAL EQUATIONS

The theoretical analysis of the circumferential flow compressor is based on the fundamental equations of continuity, momentum and energy using the assumption that the flow is steady and one dimensional. In general the following analytical work is based on the special problem, "An Experimental and Theoretical Investigation of the Peripheral Drag Compressor", by D. P. Traviss.[10]

Consider the volume element as shown below.

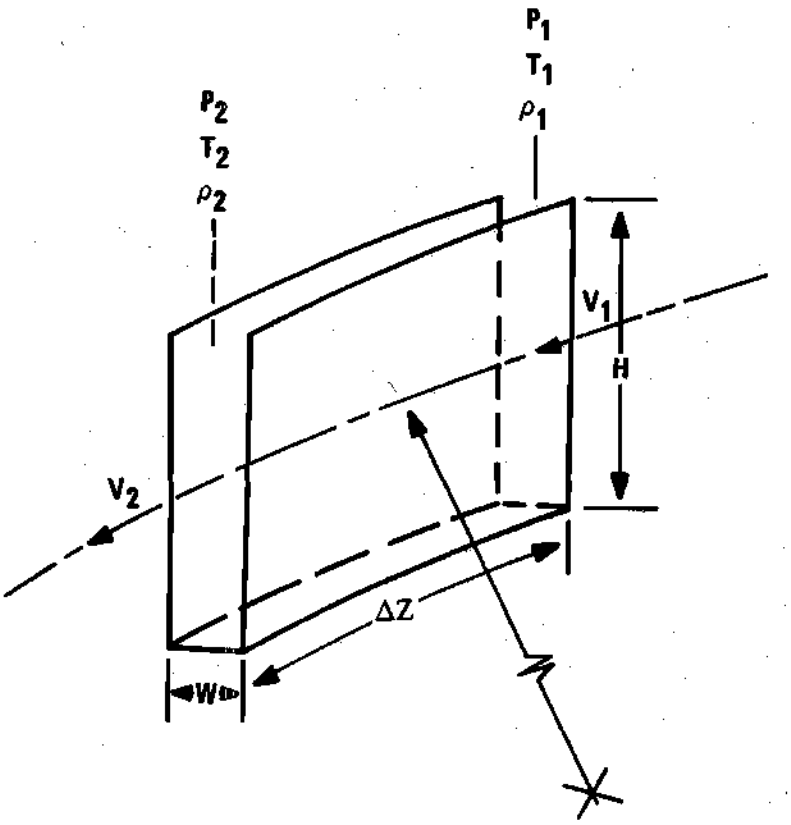

Figure 3-1. Elemental Control Volume.

3-1. Continuity Equation

The continuity equation for a control volume is:

$$\frac{\partial}{\partial t}\int_{C.V.} \rho dv = -\int_{A} \rho(\vec{V}-\vec{V}_{C.V.})\cdot\vec{n}dA \quad . \tag{1}$$

For a stationary volume element, assuming the flow to be steady and one dimensional,

$$\rho_1 V_1 A_1 = \rho_2 V_2 A_2 = \dot{M} \quad . \tag{2}$$

3-2. Momentum Equation

The momentum equation for a control volume is

$$\Sigma F = \frac{\partial}{\partial t}\int_{C.V.} \rho V dv + \int_{A} \rho\vec{V}(\vec{V}-\vec{V}_{C.V.})\cdot\vec{n}dA \quad . \tag{3}$$

For a stationary volume element, assuming the flow to be steady and one dimensional, a force balance on the elemental control volume yields:

$$\Sigma F = \tau_o A_W - \Delta P A_C = \frac{\dot{M}}{g_c}(V_2-V_1) \tag{4}$$

where

$$A_W = (2H + W)\Delta Z \tag{5}$$

$$A_C = HW \tag{6}$$

$$\Delta P = P_2 - P_1 \tag{7}$$

$$\tau_o = \frac{f\rho V^2}{8g_c} \quad . \tag{8}$$

Substituting equation (5), (6), (7) into (4) and rearranging yields:

$$P_2 = \left[\frac{\tau_o(2H+W)\Delta Z}{HW} + P_1 + \frac{\dot{M}V_1}{R_c g_c HW}\right] - \left[\frac{\dot{M}}{R_c g_c HW}\right] V_2 \quad . \tag{9}$$

3-3. Energy Equation

The energy equation for a control volume is:

$$J\dot{Q}-\dot{W} = \frac{\partial}{\partial t}\int_{C.V.} \rho\left(u + \frac{V^2}{2g_c} + gz\right)dv$$

$$+ \int_A \rho\left(h + \frac{V^2}{2g_c} + gz\right)(V-V_{C.V.})n.dA \tag{10}$$

For a stationary elemental control volume, assuming the flow to be steady state, dimensional, and neglecting potential energy changes:

$$J\dot{Q}-\dot{W} = \frac{\dot{M}}{R_c}\left[\Delta h + \frac{V_2^2}{2g_c} - \frac{V_1^2}{2g_c}\right] \tag{11}$$

where

$$\dot{W} = \tau_o(2H+W)(\Delta z)u \quad . \tag{12}$$

Substituting equation (12) into (11), and considering the fluid to be perfect gas yields:

$$J\dot{Q} + \tau_o(2H+W)\Delta zu$$

$$= JC_p\left(\frac{P_2HWV_2}{R} - \frac{P_1HWV_1}{R}\right) + \frac{\dot{M}}{2R_c g_c}(V_2^2-V_1^2) \quad . \tag{13}$$

3-4. Wall Shear Stress

Let the velocity of the fluid relative to the rotor slot be

$$V_f/r = (u-V) \quad .$$

Then Reynold's number basis on hydraulic diameter[2] is

$$R_e = \frac{\rho(u-V)(2HW)}{\mu(H+W)} \quad . \tag{14}$$

The variation of the absolute fluid viscosity with temperature[2] is

$$\mu = \mu_o\left(\frac{I}{T_o}\right)^m$$

where m is 0.712 for the temperature range of 500°R to 1000°R.

Use

$$f = \frac{0.316}{Re^{\frac{1}{4}}}, \quad 2 \times 10^3 < Re < 1 \times 10^6 \tag{17}$$

$$f = \frac{71}{Re}, \quad 100 < Re < 2000 \tag{18}$$

and take the wall shear stress to be

$$\tau_o = \frac{f\rho V^2}{8g_c} \quad . \tag{19}$$

3-5. Method of Solution

The momentum equation (9) can be written in the form

$$P_2 = C_1 - C_2V_2 \quad . \tag{20}$$

Substituting equation (20) in to the energy equation (13) and

rearranging,

$$\left[\frac{\dot{M}}{2g_c(R_cHW)} - \frac{JC_{p_2}}{R}\right]V_2^2 + \left[\frac{JC_{p_1}}{R}\right]V_2$$

$$- \left[\frac{JQ}{\dot{M}W} + \tau_o\left(\frac{2H+W}{W}\right)\Delta zu + \frac{JC_{p_1}P_1V_1}{R} + \frac{\dot{M}V_1^2}{2g_c(RHW)}\right] = 0 \quad . \tag{21}$$

From the ideal gas assumption and the continuity equation,

$$T_2 = \frac{P_2}{\rho_2 R} \tag{22}$$

and

$$\rho_2 = \frac{\dot{M}}{V_2(RHW)} \quad .$$

Thus, when the specific geometry (R, H, W, Z), mass flow rate ($\dot{M}$), wheel speed (u), and entrance conditions (P_1, T_1, ρ_1) are known, the exit conditions (P_2, T_2, ρ_2, V_2) can be determined.

The conditions in the nozzle exit are considered to be isentropic and determined by the equation[1],

$$\frac{\dot{M}\sqrt{T_o}}{P_o A} = \frac{K}{R} \cdot \frac{M}{\left(1 + \frac{K-1}{2} M^2\right)^{\frac{K+1}{2(K-1)}}} \quad .$$

This equation was solved for the mass flow parameter $\frac{\dot{M}\sqrt{T_o}}{P_o A}$ as a function of the Mach number for the range $0 \leq M \leq 1$.

Traviss has solved these equations on a digital computer by dividing the arc length of the compressor passage into ten segments. The logic diagram and computer program are in Appendix A-1 and Appendix A-2

respectively. A typical computer run for 42,000 rpm, is shown in Appendix A-3.

CHAPTER IV

RESULTS

4-1. The Experimental Limit

Initially the test program called for running the compressor to a maximum speed of 70,000 RPM, however, due to a limit on power of the turbine drive and vibration of the compressor wheel at high speed, data were obtained to a maximum speed of only 42,000 RPM. Also at higher speeds seal difficulties began to cause considerable operating trouble. Evidence of seal wear and breakage is indicated in Figure 4-1.

4-2. Theoretical Curve and Theoretical Limit

From the analytical work, a set of theoretical curves for speeds from 15,000 to 70,000 RPM are shown in Figure 4-2. The nozzle at the inlet of the compressor becomes choked at a flow rate of 63.3 SCFM.

4-3. Comparison Between Experiment and Theory

Leakage between the seal and the wheel, and wheel and casing has a great effect on the pressure rise of the compressor. Figures 4-3 and 4-4 are experimental curves for two pairs of seals. Figure 4-3 indicates higher pressure rises for corresponding flow rates and rotor speeds than does Figure 4-4. The seals used in obtaining the data presented in Figure 4-4 had some tips broken and the gasket between the wheel and casing did not fit well. Figure 4-4 at 30,000 RPM also indicates that after the seals were readjusted, the compressor gave higher pressure

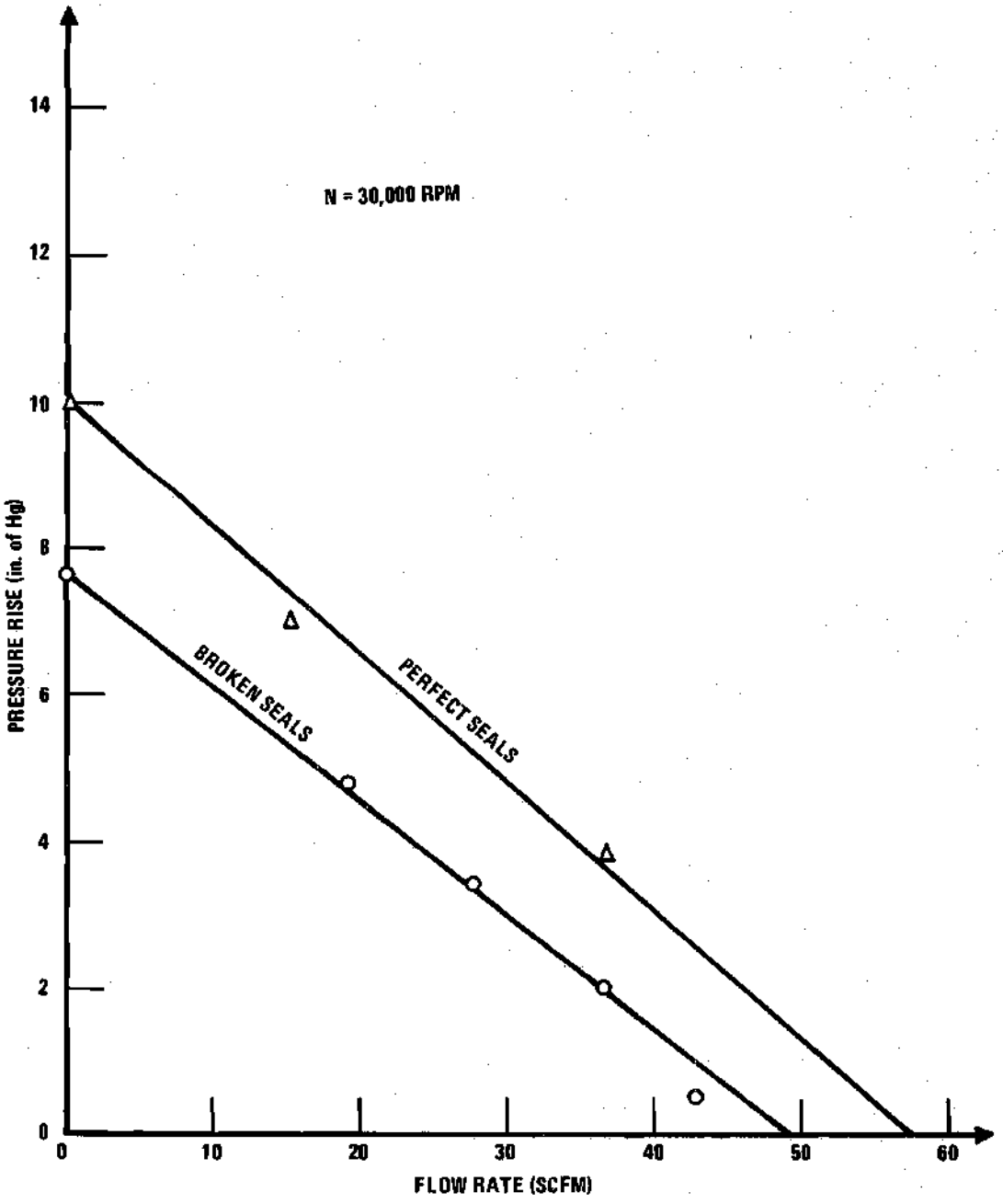

Figure 4-1. Comparison Between Perfect and Broken Seals Because of High Speed

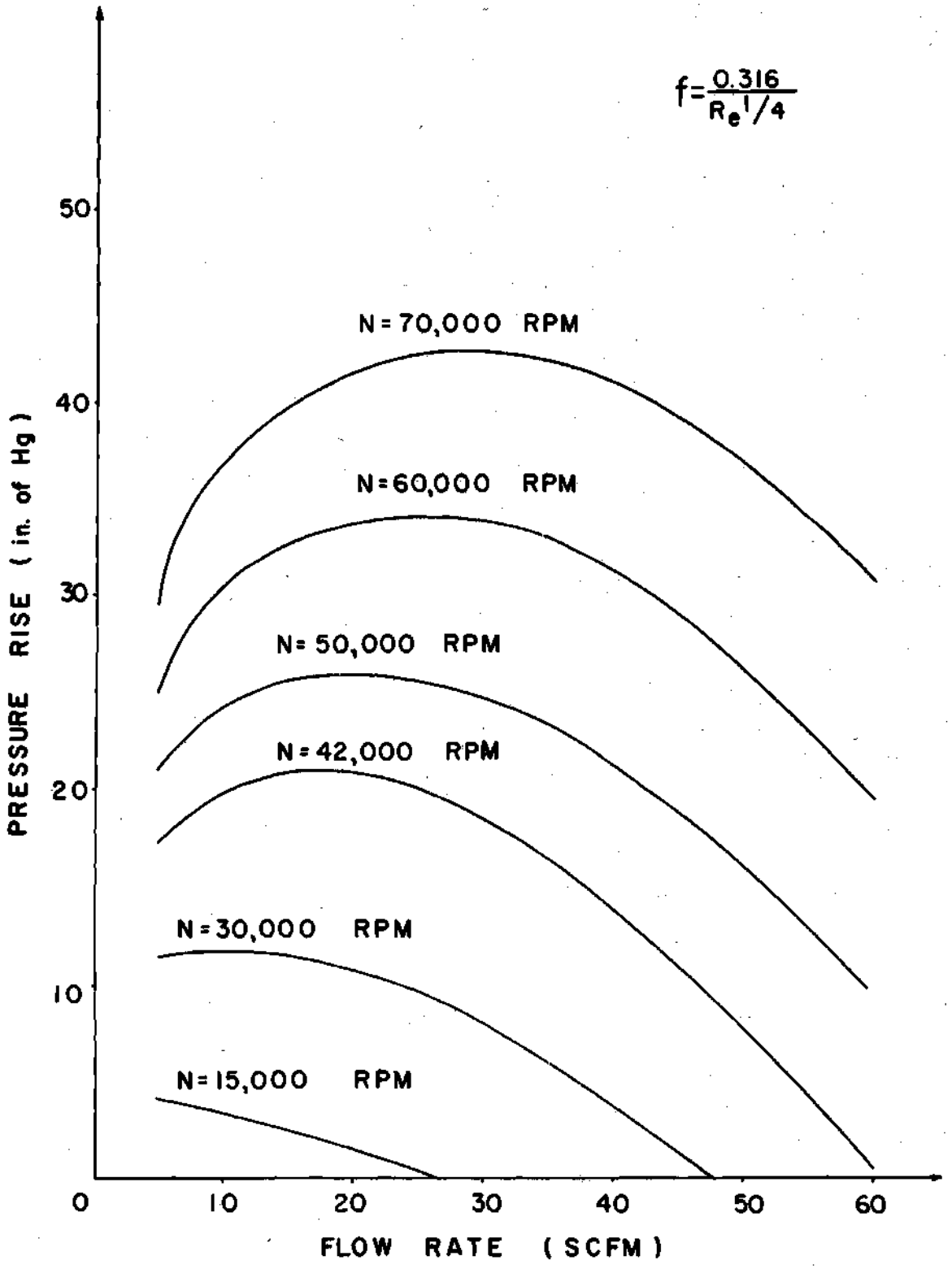

Figure 4-2. Theoretical Pressure Rise vs. Flow Rate

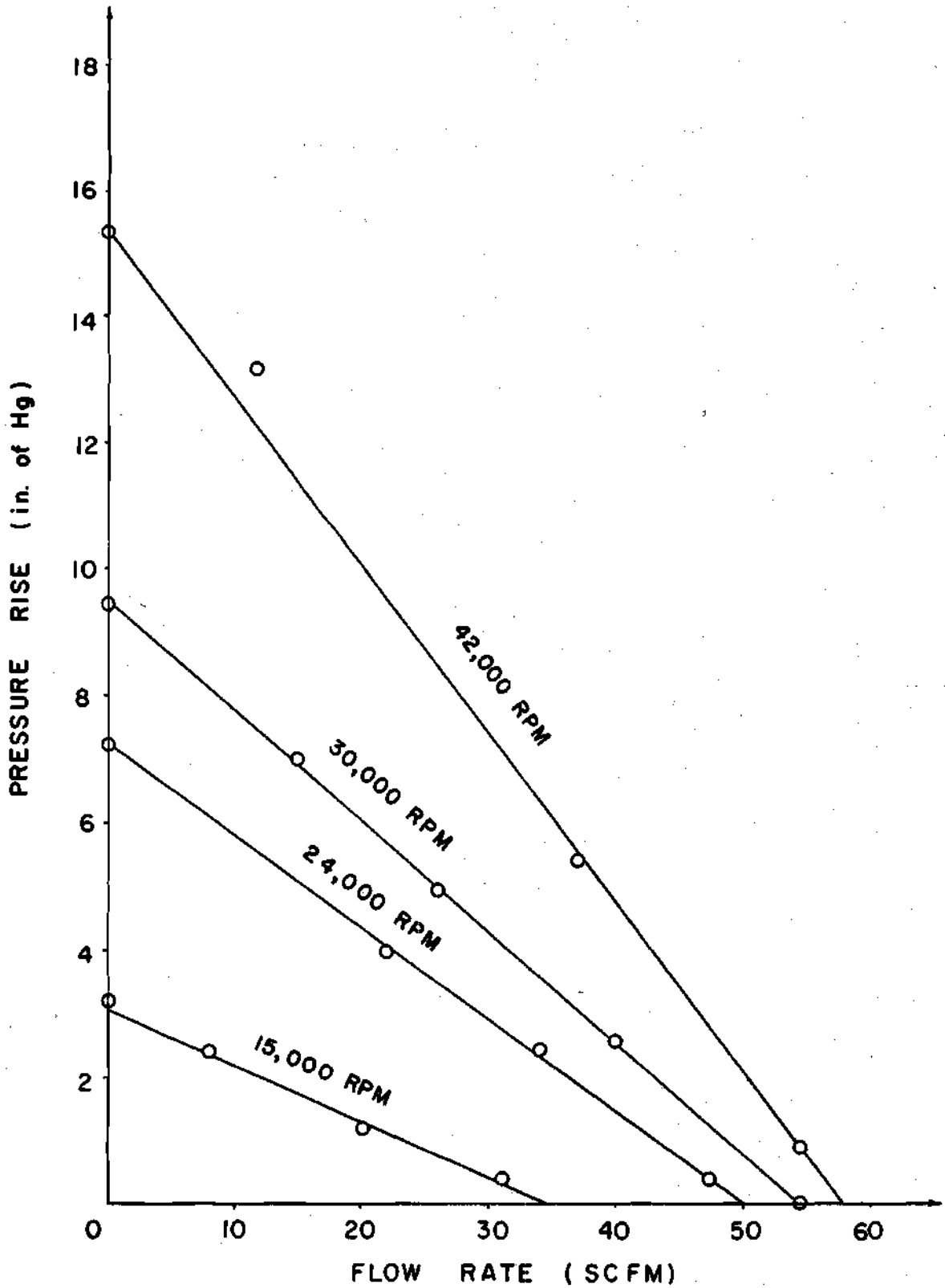

Figure 4-3. Experimental Pressure Rise vs. Flow Rate

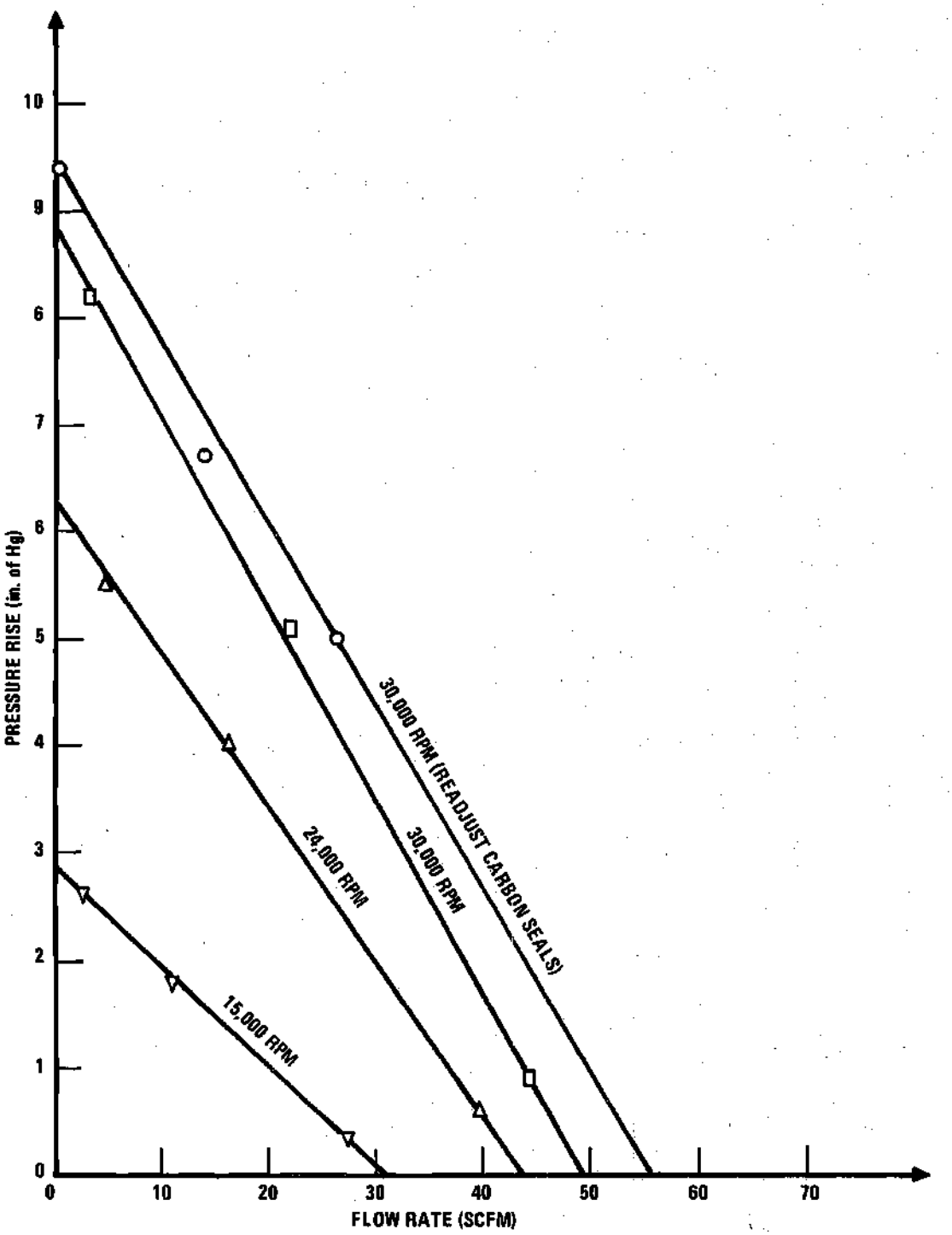

Figure 4-4. Experimental Pressure Rise vs. Flow Rate

rises for the same operating conditions. However, performance was still lower than that shown in Figure 4-3 because of poor gaskets.

All of the experimental curves obtained show pressure rises lower than the theoretical curves for the same flow rates and rotor speeds. This may be the friction factor used for the theoretical curves was the friction factor for a circular duct. An attempt was made to obtain better agreement by changing the constant in the friction factor equation. Taking the friction factor to be $0.2/Re^{\frac{1}{4}}$ rather than the pipe value of $0.316/Re^{\frac{1}{4}}$ gave better agreement between calculations and measurements as indicated in Figures 4-5 and 4-6. From the data it is evident the experimental curves are nearly linear while the theoretical curves exhibit considerable curvature. The flow process was assumed to be adiabatic and leakage was neglected in the theoretical calculations. Thus heat transfer and leakage may be two major reasons for the lack of agreement between theory and experiment.

4-4. Temperature Profile

In this section and in all the following sections $f = 0.2/Re^{\frac{1}{4}}$ has been used in computing the theoretical curves. Comparison between theoretical and experimental outlet temperatures for each rotor speed are shown in Figures 4-7 to 4-10. For low flow rates, the theoretical outlet temperature are higher, while for high flow rates the experimental temperatures are higher. Heat transfer would cause exit temperature to be lower than the theoretical values predicted using the adiabatic assumption. Thus heat transfer effects tend to explain the differences between theory and experiment at low flow rate. However, heat transfer

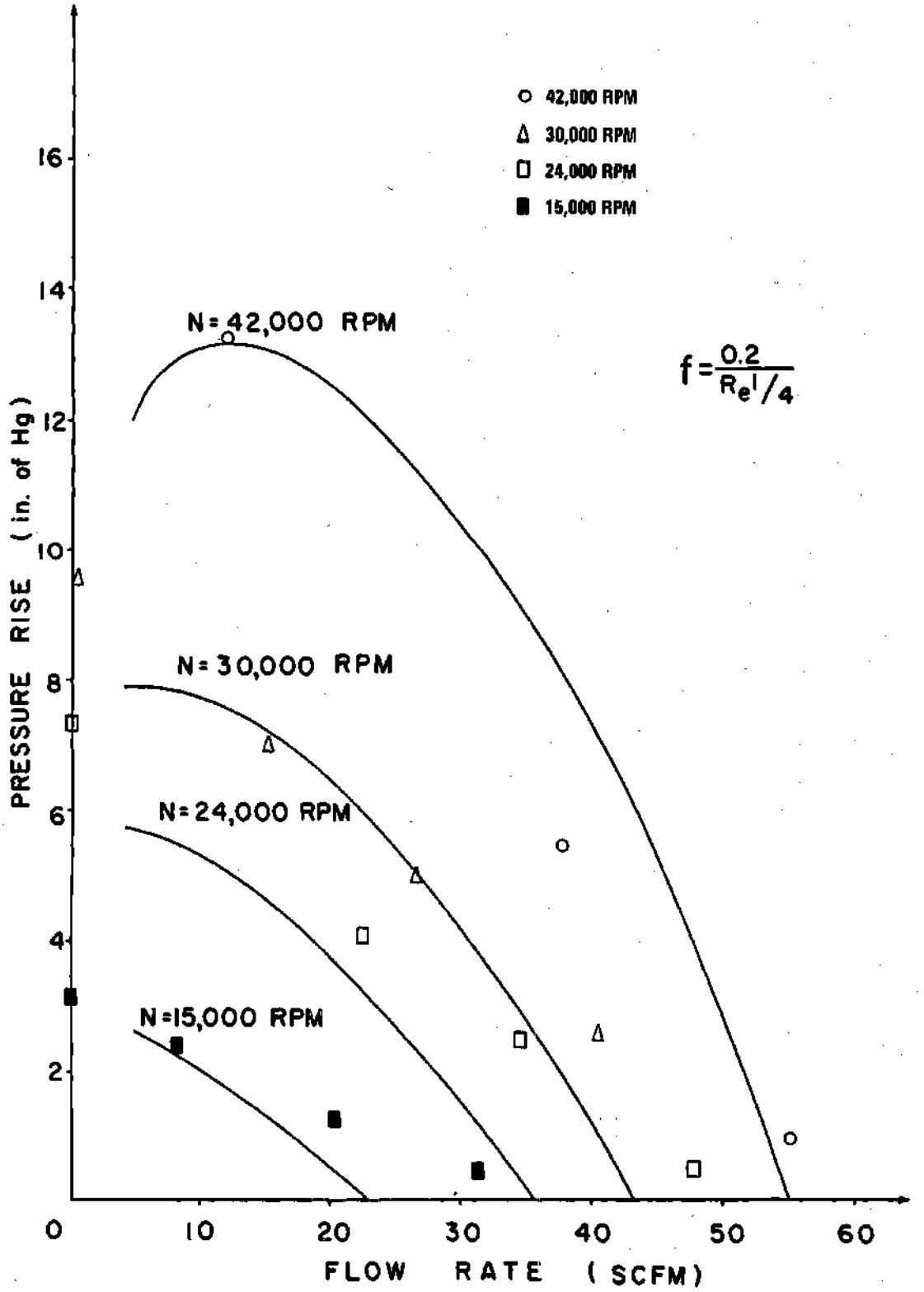

Figure 4-5. Theoretical Pressure Rise vs. Flow Rate

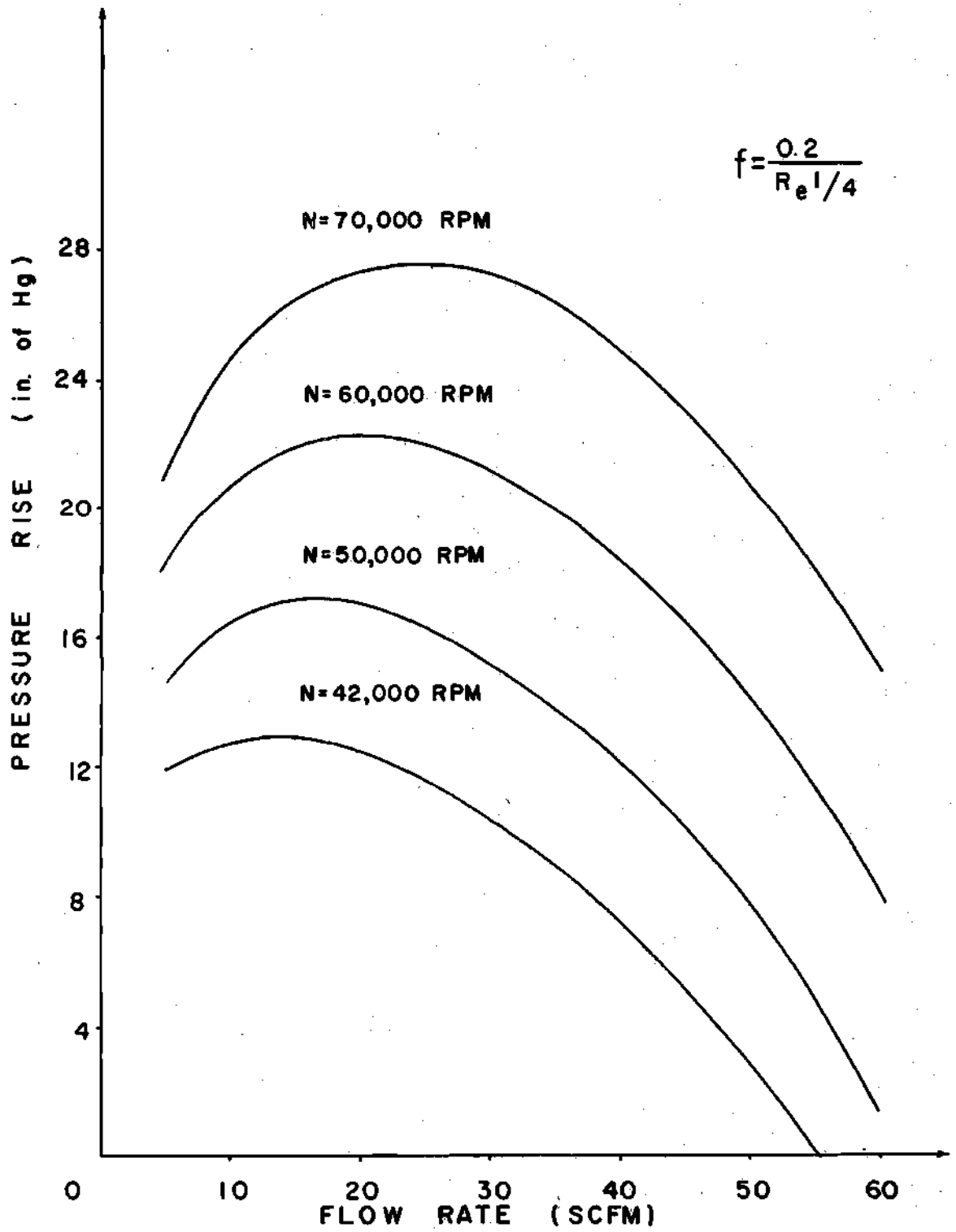

Figure 4-6. Theoretical Pressure Rise vs. Flow Rate

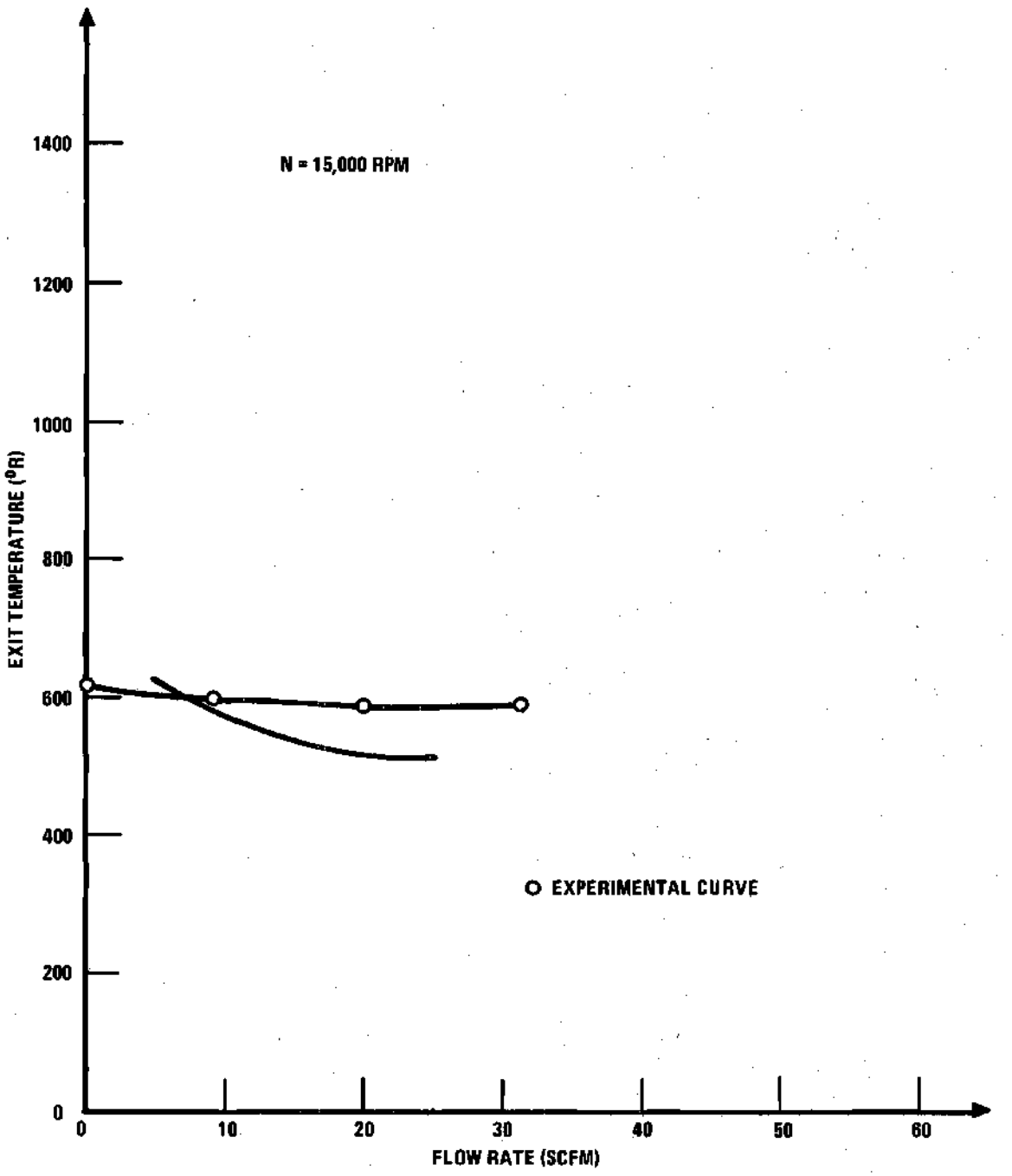

Figure 4-7. Exit Temperature vs. Flow Rate

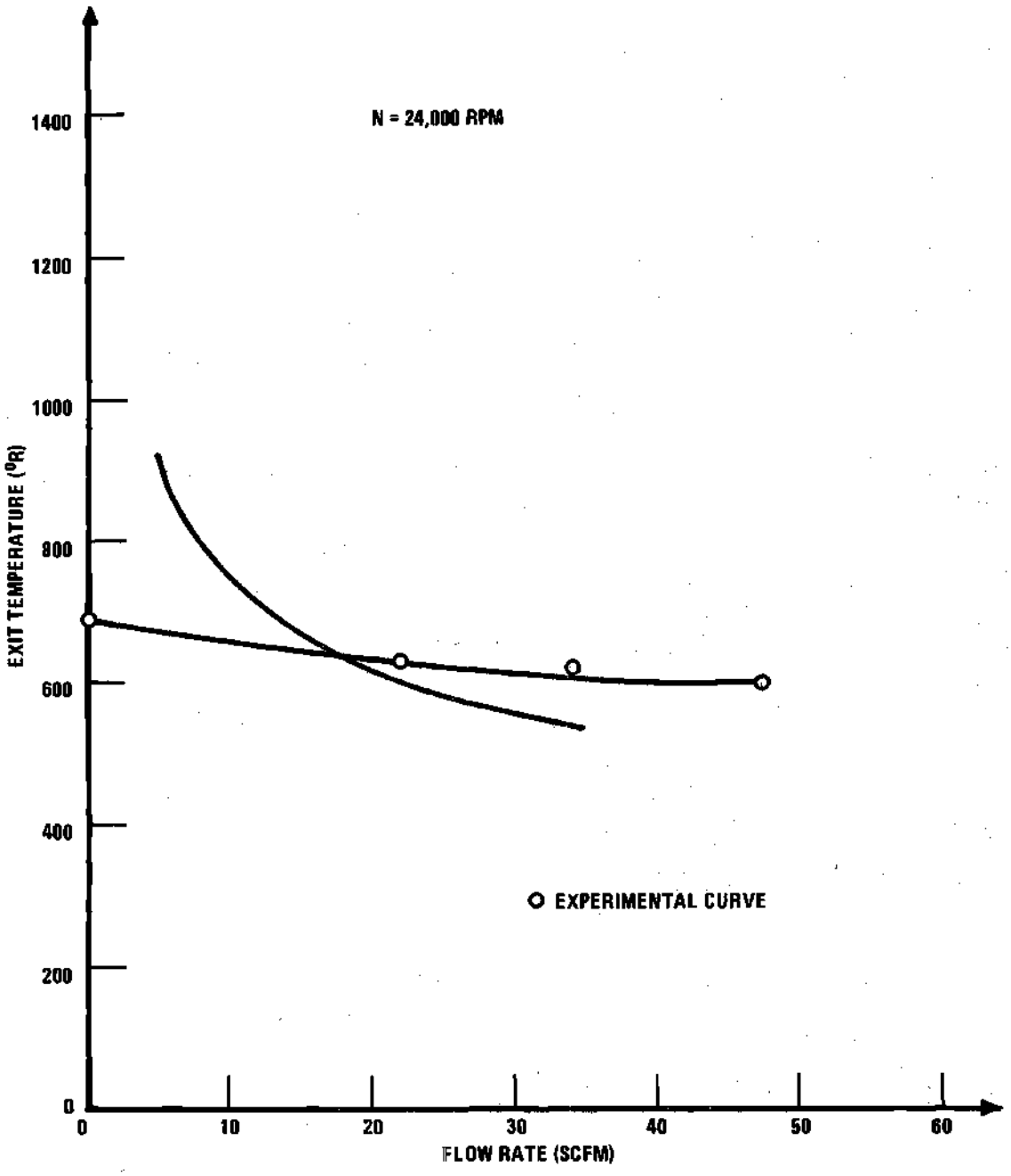

Figure 4-8. Exit Temperature vs. Flow Rate

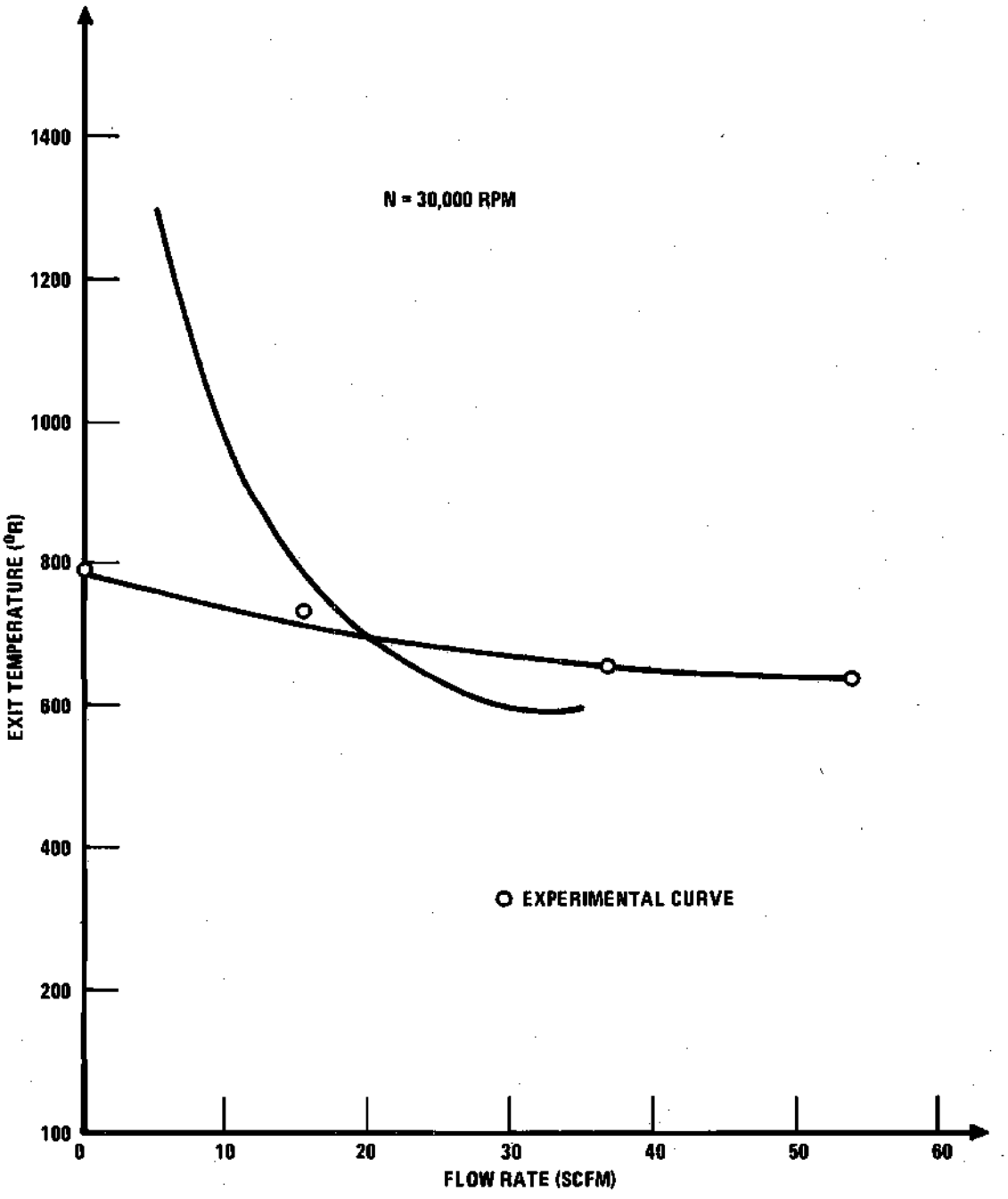

Figure 4-9. Exit Temperature vs. Flow Rate

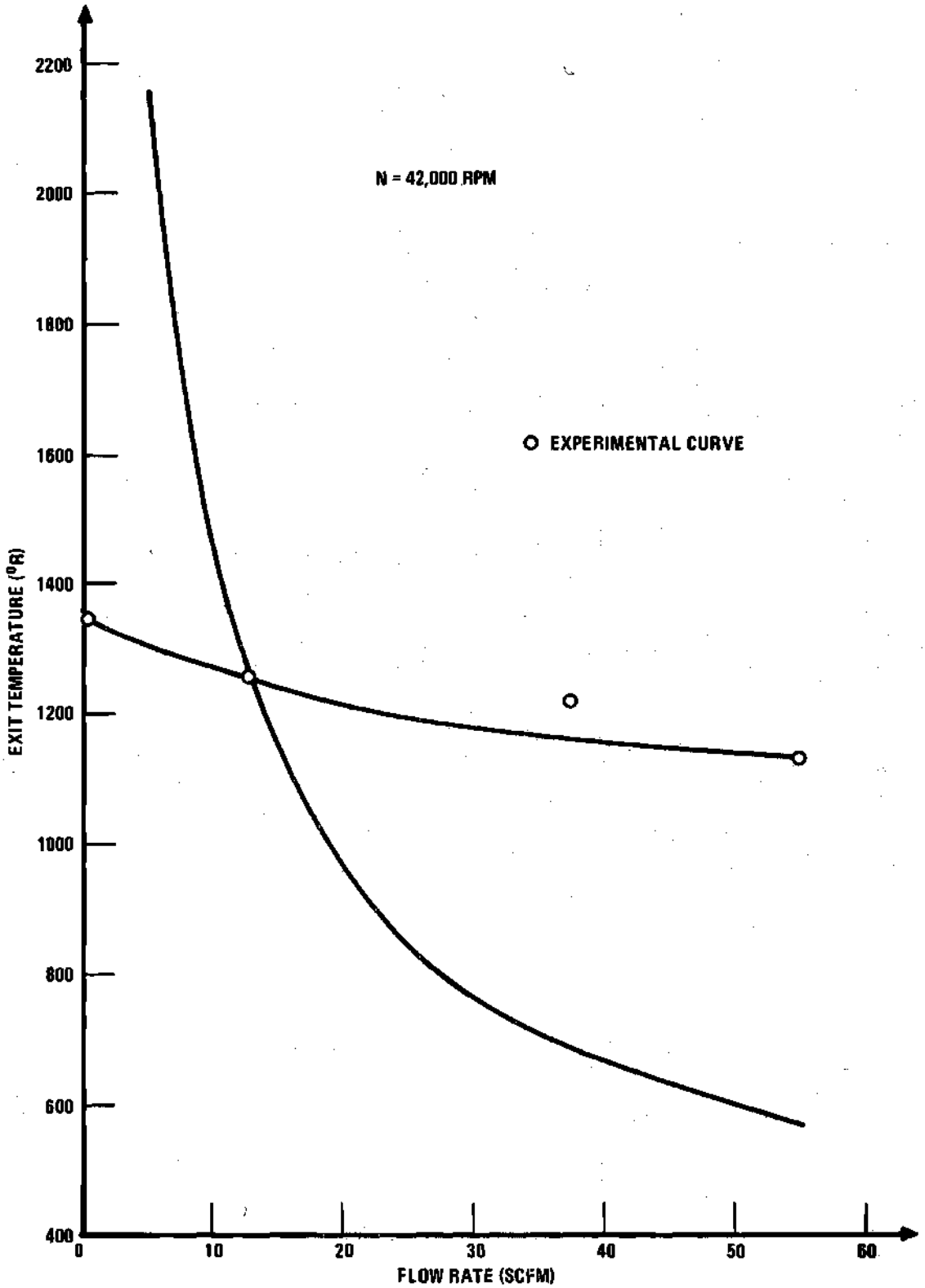

Figure 4-10. Exit Temperature vs. Flow Rate

cannot account for the differences shown at high flow rate. Apparently more turbulence exists than is accounted for with the friction factor chosen. Curvature effects may also contribute to the difference noted.

Experimental ambient, inlet, outlet and laminar flow element temperatures versus flow rate are shown in Figures 4-11 to 4-13.

4-5. Theoretical Pressure and Velocity Along the Arc

Results of a theoretical pressure study along the arc of the compressor are shown in Fig. 4-14 and 4-15 for N = 30,000 RPM and 42,000 RPM respectively. The pressure rise is linear and varies inversely with the mass flow rate. At high flow rates at each rotor speed, inlet velocity is very high and hence negative pressure is developed at the entrance.

Figures 4-16 and 4-17 show theoretical velocities along the arc. Velocity is increased for low flow rates at each rotor speed. At these low flow rates, for all rotor speeds temperature rises are very high, consequently, because mass flow rate and area are constant and density varies inversely with temperature, velocity is increased along the arc. At flow rates of 25 and 35 SCFM for rotational speeds of 30,000 and 42,000 RPM respectively, the velocity is constant along the arc. Thus for these flow rates and rotor speeds, the fluid momentum is constant, indicating that the drag force on the fluid is balanced by the adverse pressure gradient.

4-6. Efficiency

The adiabatic compression efficiency[5] is defined as the theoretical power required assuming isentropic compression divided by the

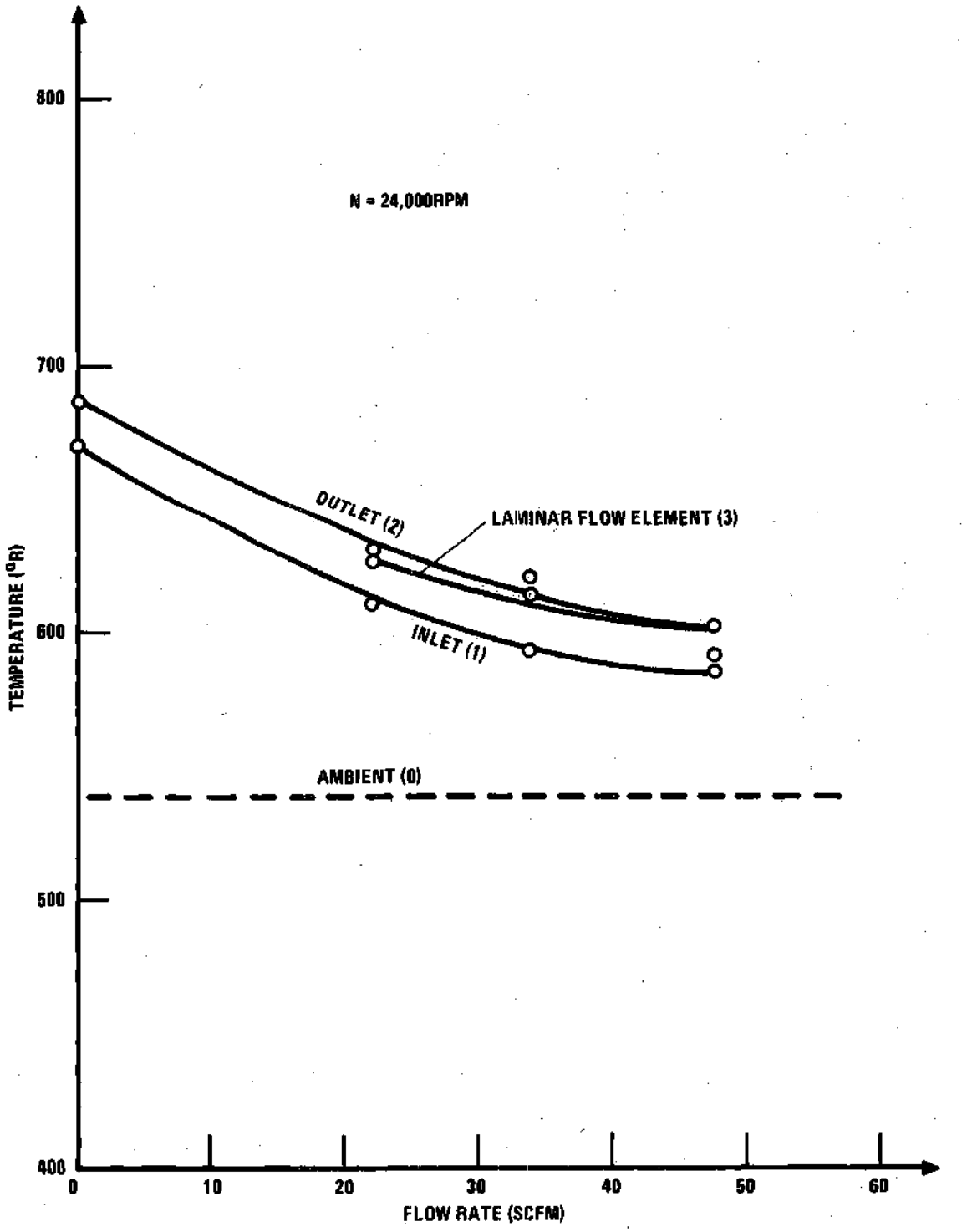

Figure 4-11. Ambient (0), Inlet (1), Outlet (2), Laminar Flow Element Temperature (3) vs. Flow Rate

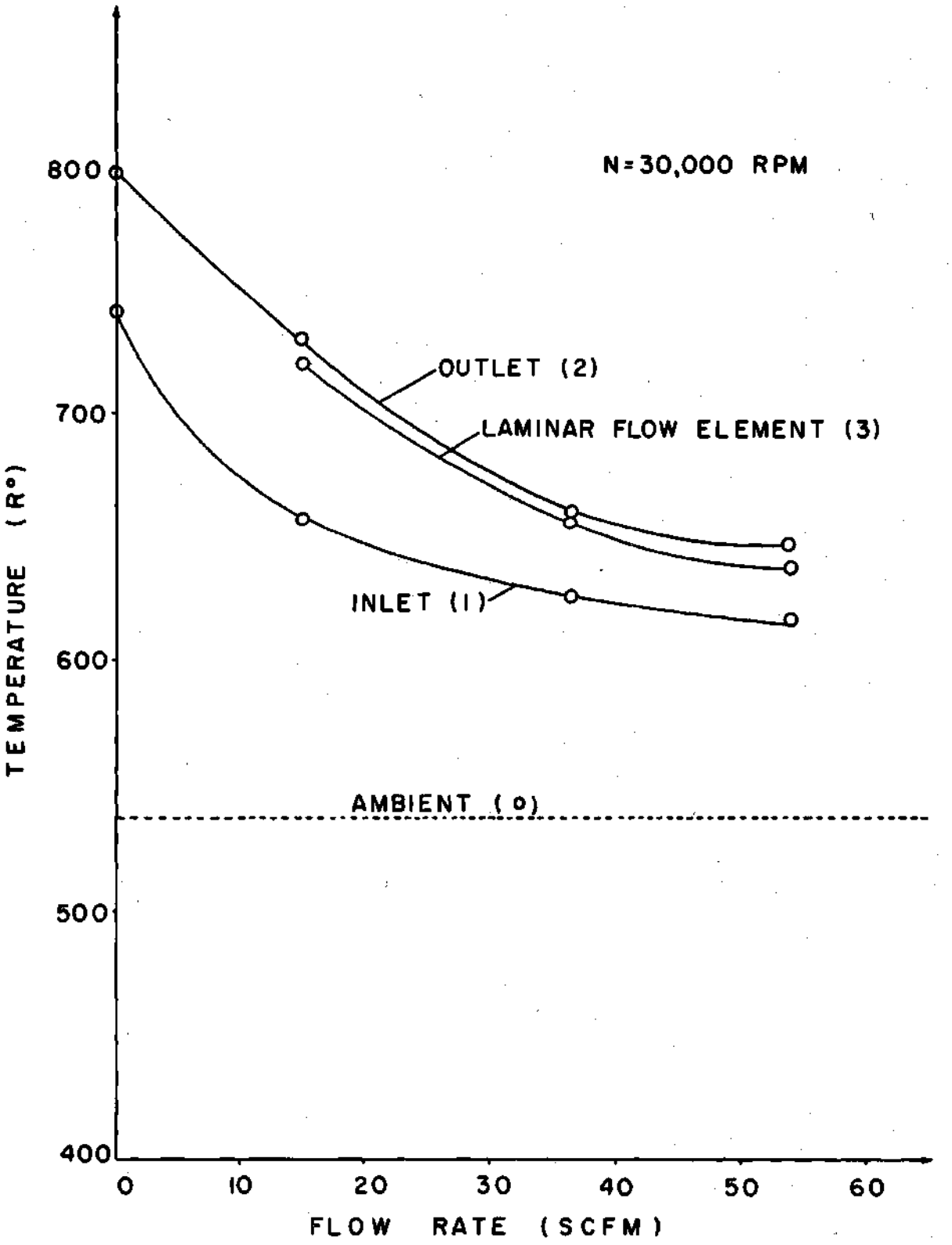

Figure 4-12. Ambient (0), Inlet (1), Outlet (2), Laminar Flow Element Temperature (3) vs. Flow Rate

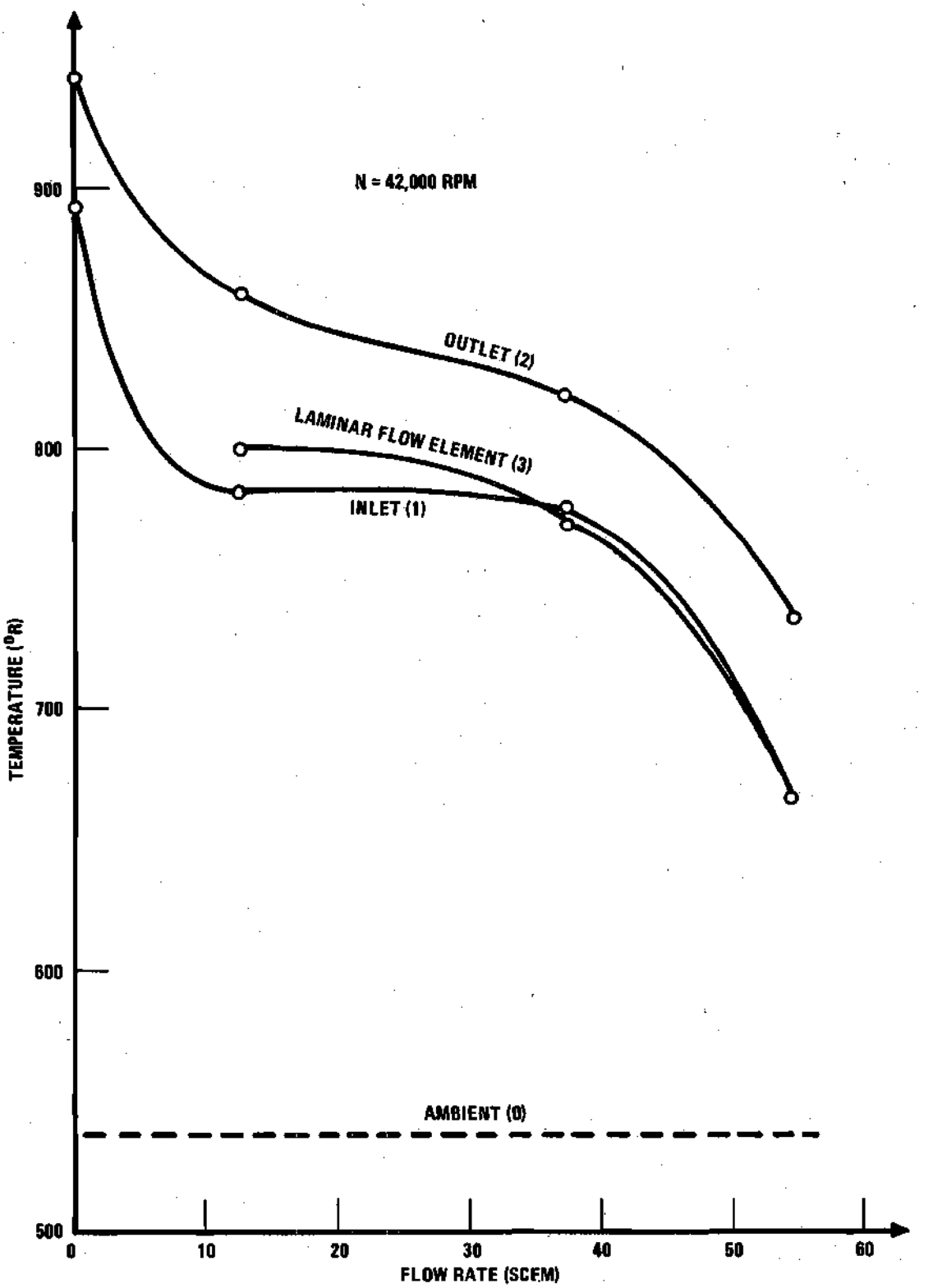

Figure 4-13. Ambient (0), Inlet (1), Outlet (2), Laminar Flow Element Temperature (3) vs. Flow Rate

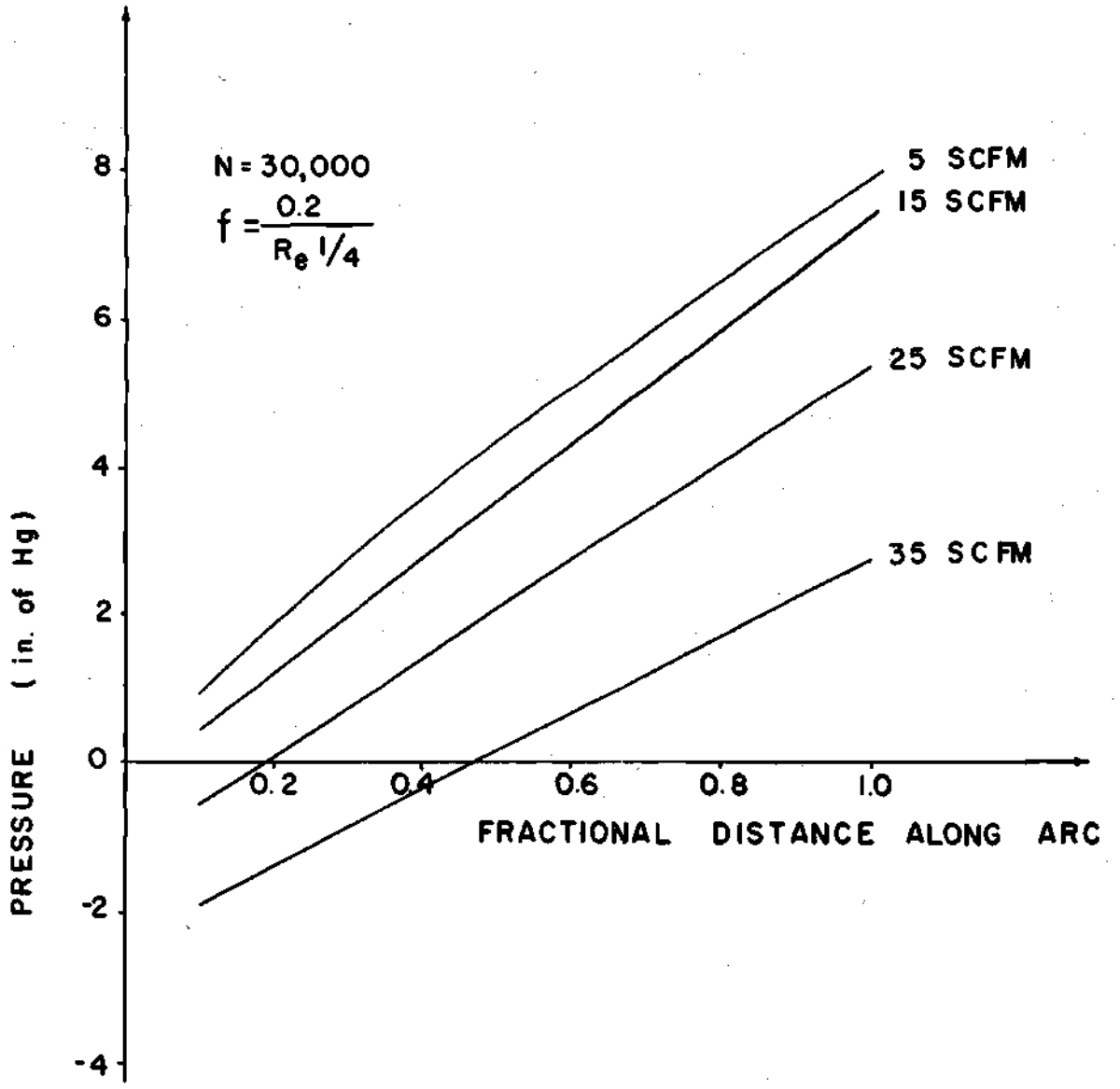

Figure 4-14. Theoretical Pressure Rise Along Arc

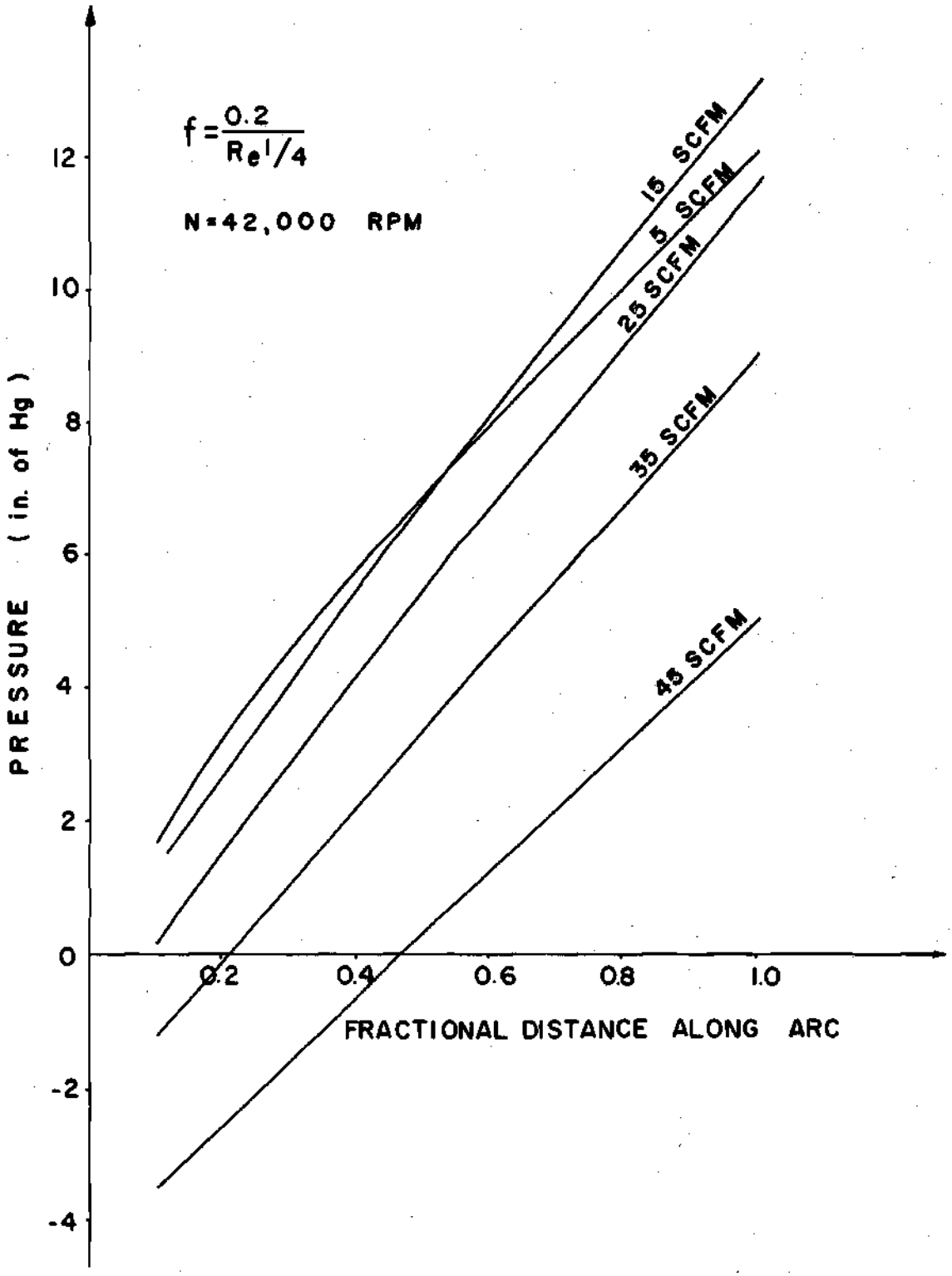

Figure 4-15. Theoretical Pressure Rise Along Arc

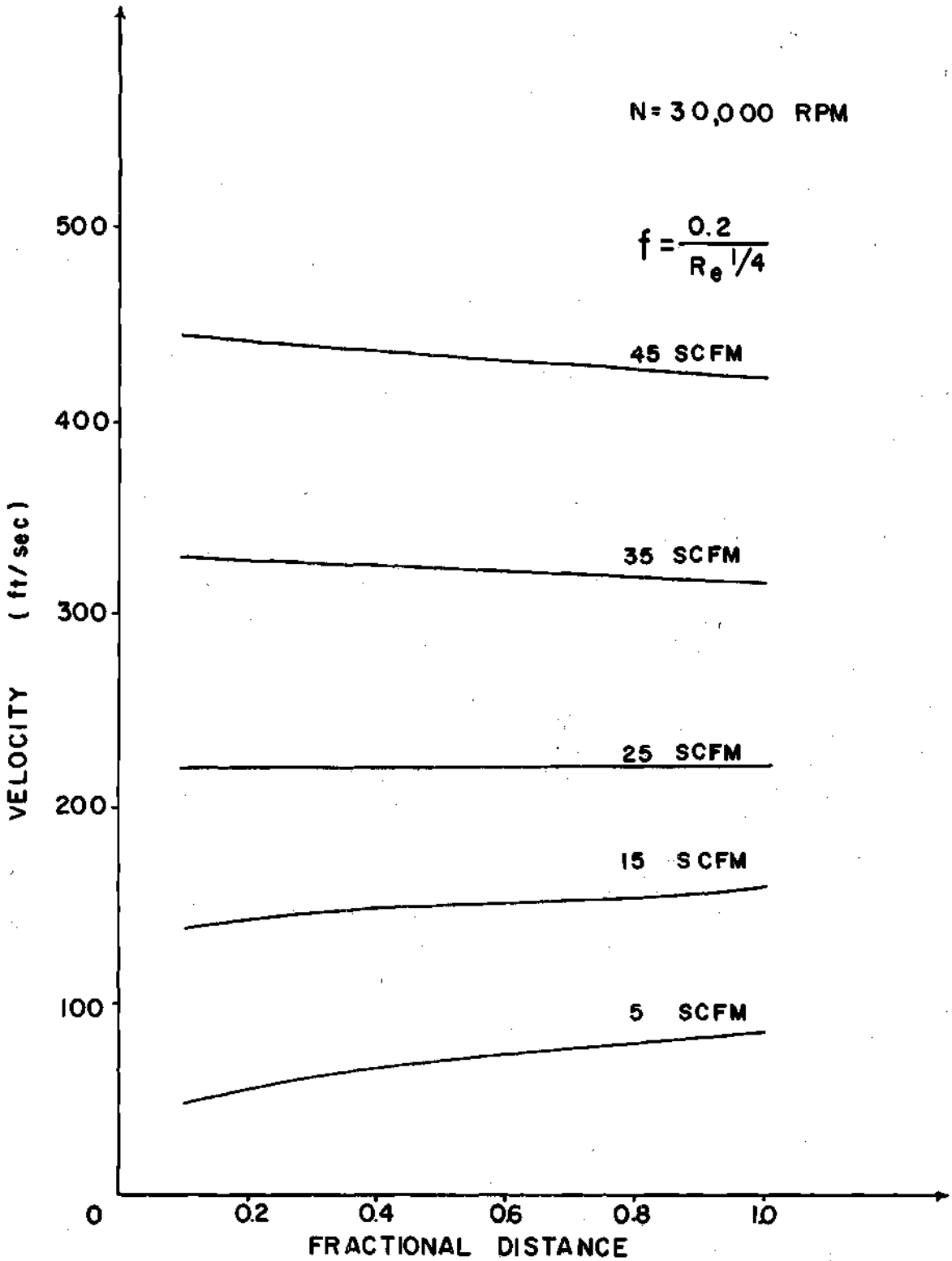

Figure 4-16. Theoretical Velocity Along Arc

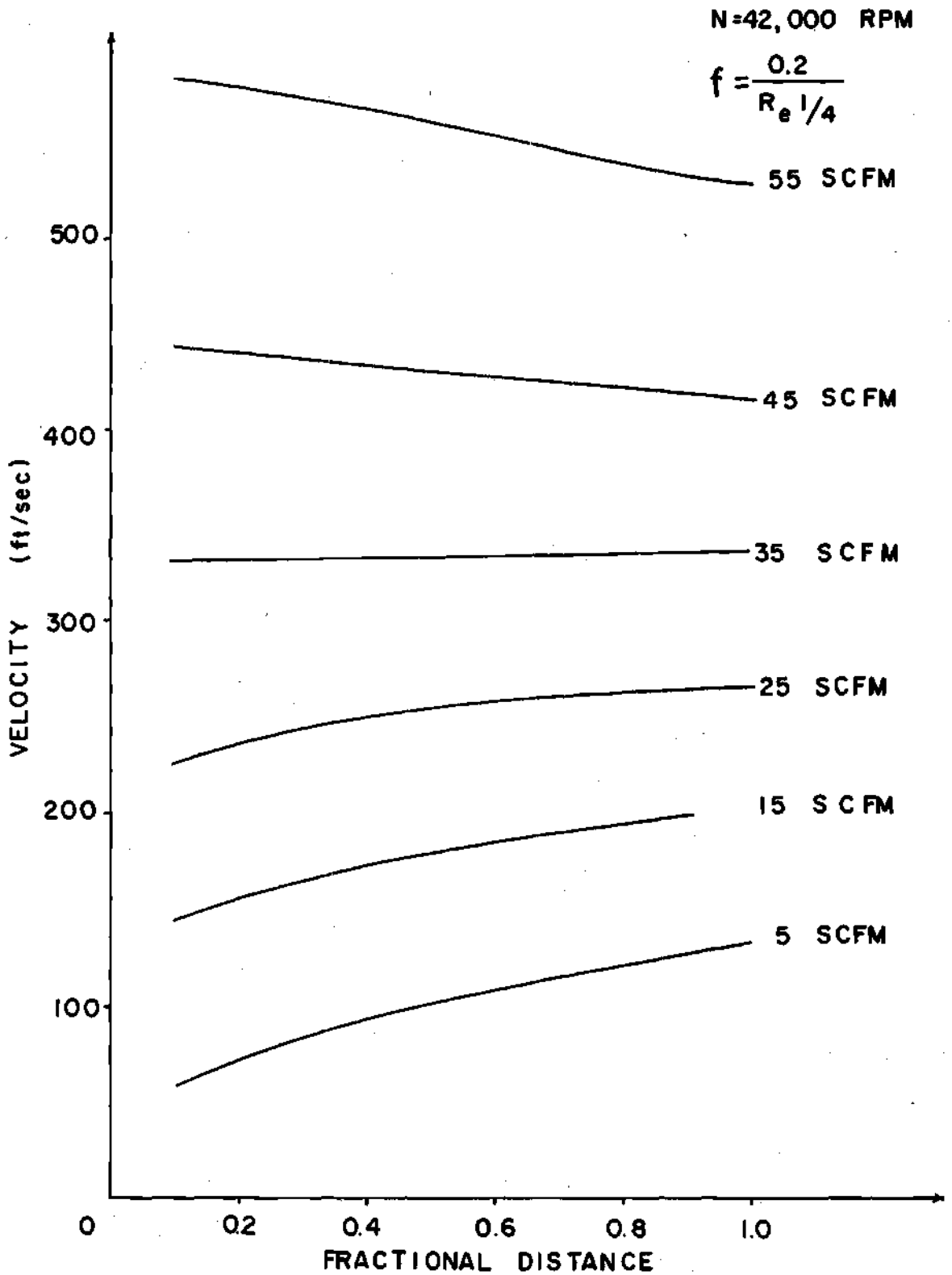

Figure 4-17. Theoretical Velocity Along Arc

actual power required by the compressor. Mathematically

$$\eta = \frac{\text{work assuming isentropic compression}}{\text{actual work of compressor}}$$

$$= \frac{C_{p_s}[Ts-To]}{C_{p_a}[Ta-To]}$$

where Ta is actual exit temperature and

$$Ts = To\left(\frac{P_2}{P_1}\right)^{\frac{K-1}{K}} .$$

Because Ta and Ts are roughly in the same range in most cases, C_{p_s} and C_{p_a} can be assumed equal. Figure 4-18 shows the adiabatic compression efficiency at each rotor speed. It is evident that at each rotor speed maximum efficiency occurs at different flow rates. However for all rotor speeds good efficiency is obtained between 5 to 35 SCFM.

4-7. Geometry Effects

The effects of geometry changes on performance characteristics were studied by using the theoretical model. Three types of geometry changes were considered. First, height and width were kept constant while varying the number of slots. Second, the number of slots and the height were held constant while width was varied. Third, the number of slots and width were held constant while height was varied. Curves shown in Figures 4-19 to 4-21 indicate the results for N = 42,000 RPM. It is evident from Figure 4-19 that increasing the number of slots gives higher pressure rises for flow rates of more than 15 SCFM. For flow

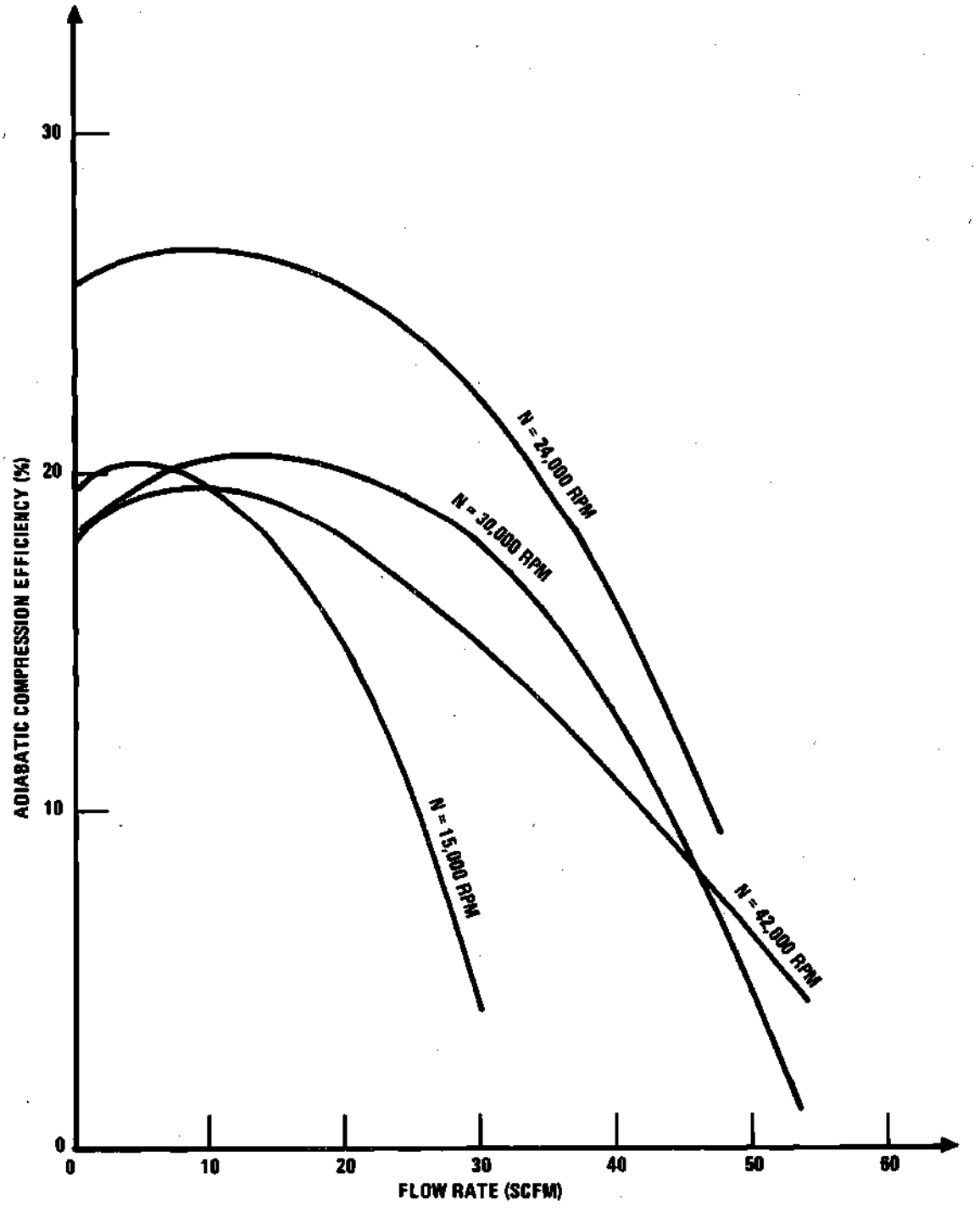

Figure 4-18. Adiabatic Compression vs. Flow Rate

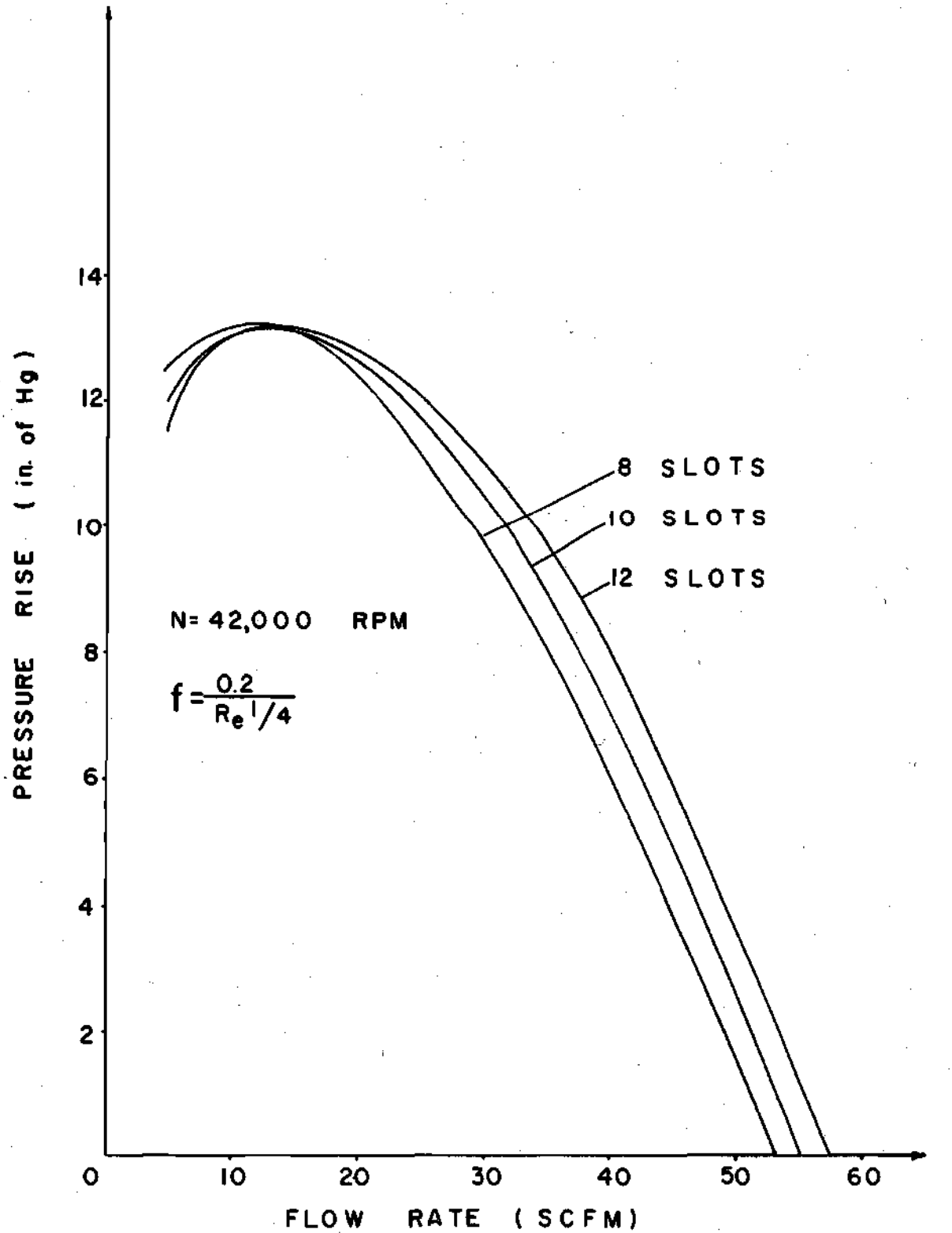

Figure 4-19. Keep Width and Height Constant Vary Number of Slots

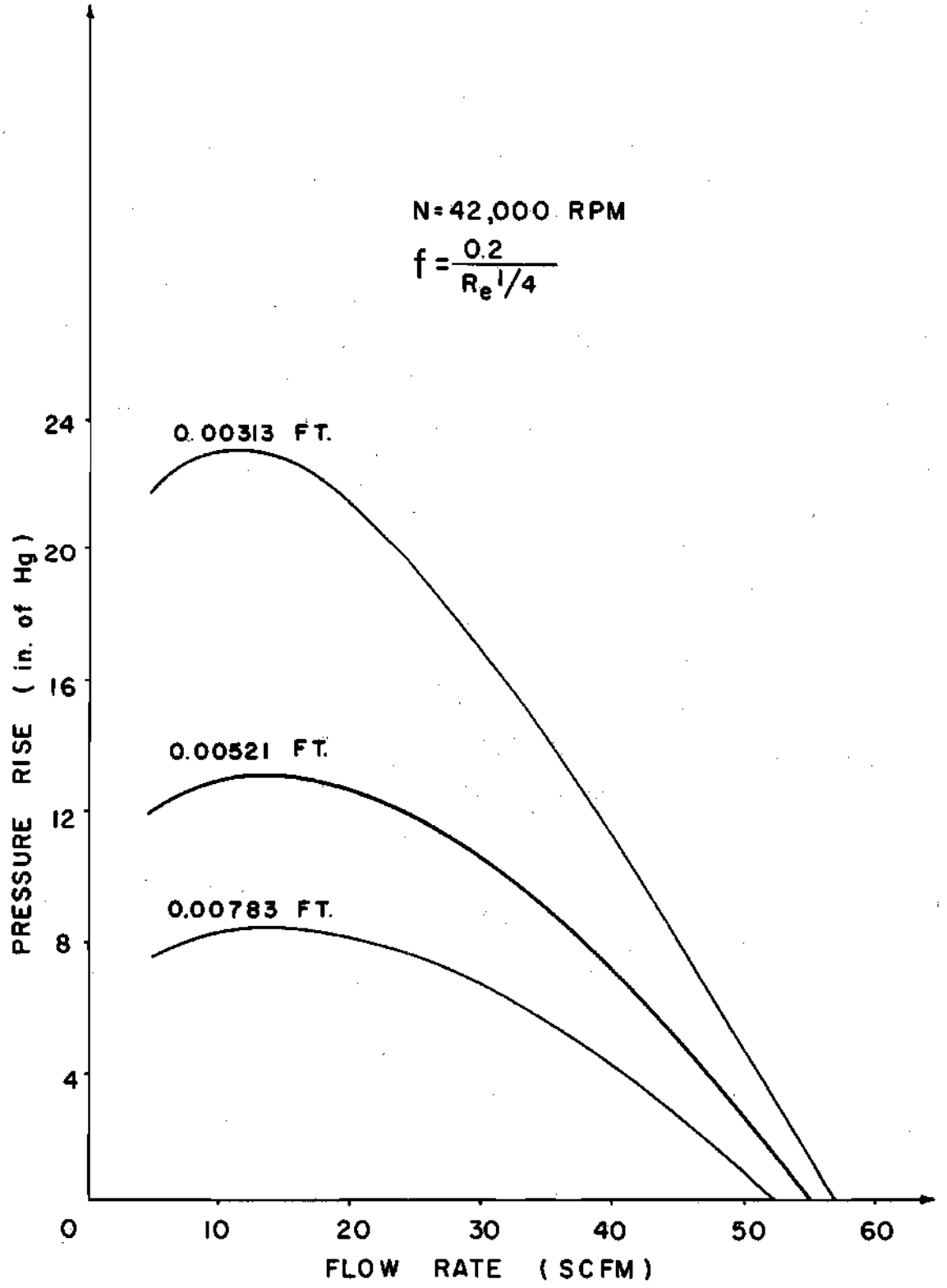

Figure 4-20. Keep Number of Slsots and Height Constant Vary Width

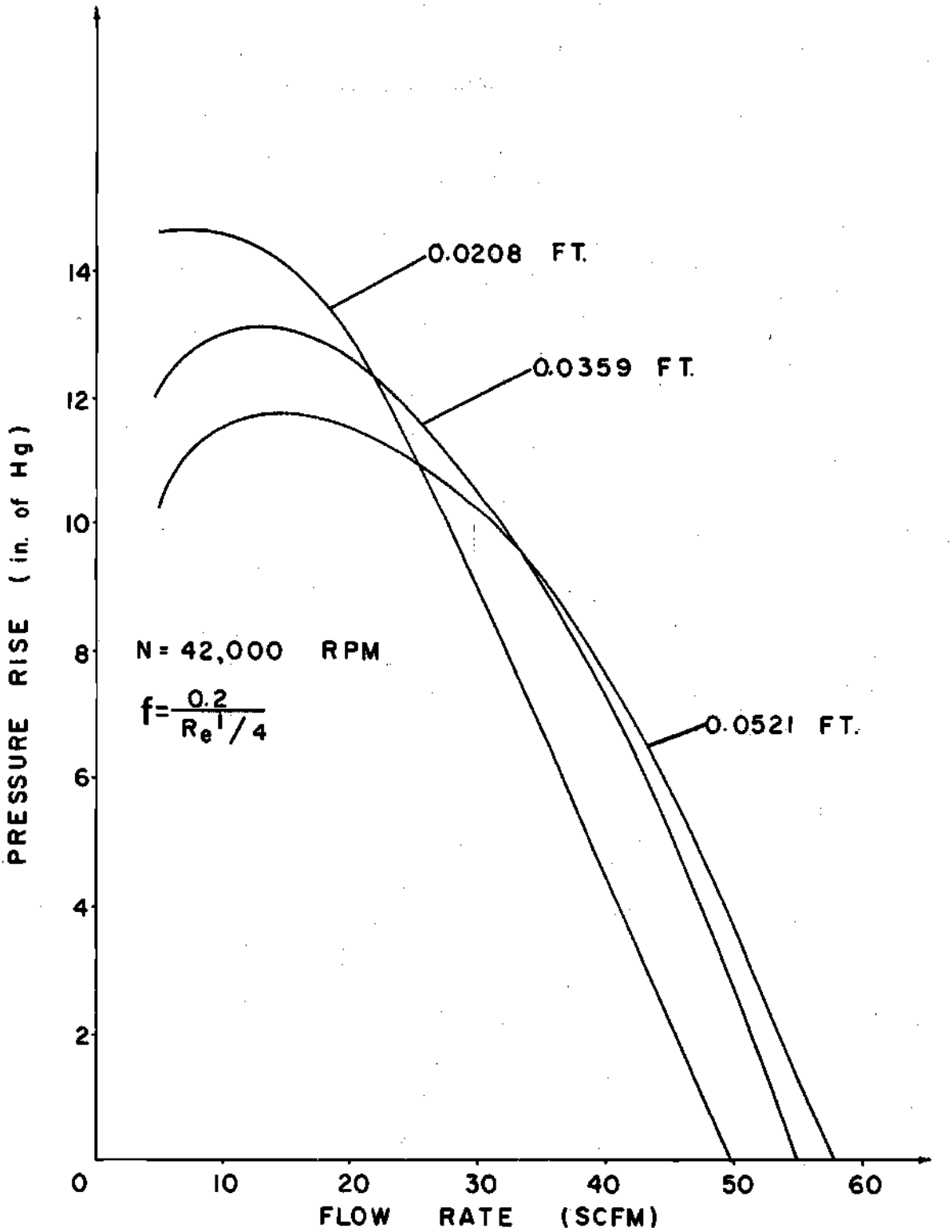

Figure 4-21. Keep Number of Slots and Width Constant Vary Height.

rates between 5 and 15 SCFM lower pressure rises are obtained. However, the compressor would seldom be operated in this region of low mass flow. Smaller widths give higher pressure as shown in Figure 4-20. Larger heights give higher pressure for high flow rates. For low flow rates greater heights cause lower pressure rises. Hence the depth of the compressor slot chosen depends on the flow rate that is required. This geometry study indicates that smaller width and the larger number of slots will give higher pressure rises.

CHAPTER V

CONCLUSIONS AND RECOMMENDATIONS

It was assumed throughout the theoretical analysis that the flow in the passages is adiabatic. However, a comparison between measured exit temperatures and calculated ones for different flow rates and speeds indicates that the flow is not adiabatic.

The friction factor $0.316/Re^{\frac{1}{4}}$ (measured for turbulent flow in smooth pipes) if used in the theoretical equations does not predict performance in agreement with measurement. The differences are probably due largely to mixing losses, leakage, and heat transfer effects. From the theoretical work it was determined that higher friction factors give higher pressures, thus a way to increase the pressure rise of the compressor is to make the surface of the wheel rough instead of smooth.

For the same flow rate, a higher speed gives a higher pressure rise. The present seal material, graphite, is too brittle and not good for high speed operation. The seal material should be resistance to high temperatures, flexible with low plastic deformation, and have a low surface resistance factor. Because titanium wheel has a high hardness; metal alloys, such as an aluminum alloy, having the characteristics mentioned above along with lower hardness, might be used for the seal instead of graphite.

From the geometry effect study, it is clear that a compressor wheel with a greater number of slots and smaller widths will give higher

pressures. The present wheel is not optimum.

It is recommended that the research effort be continued, with better designed wheels, until a wheel rim speed of approximately 2000 feet per second is reached.

APPENDICES

TABLE A–1 COMPUTER LOGIC

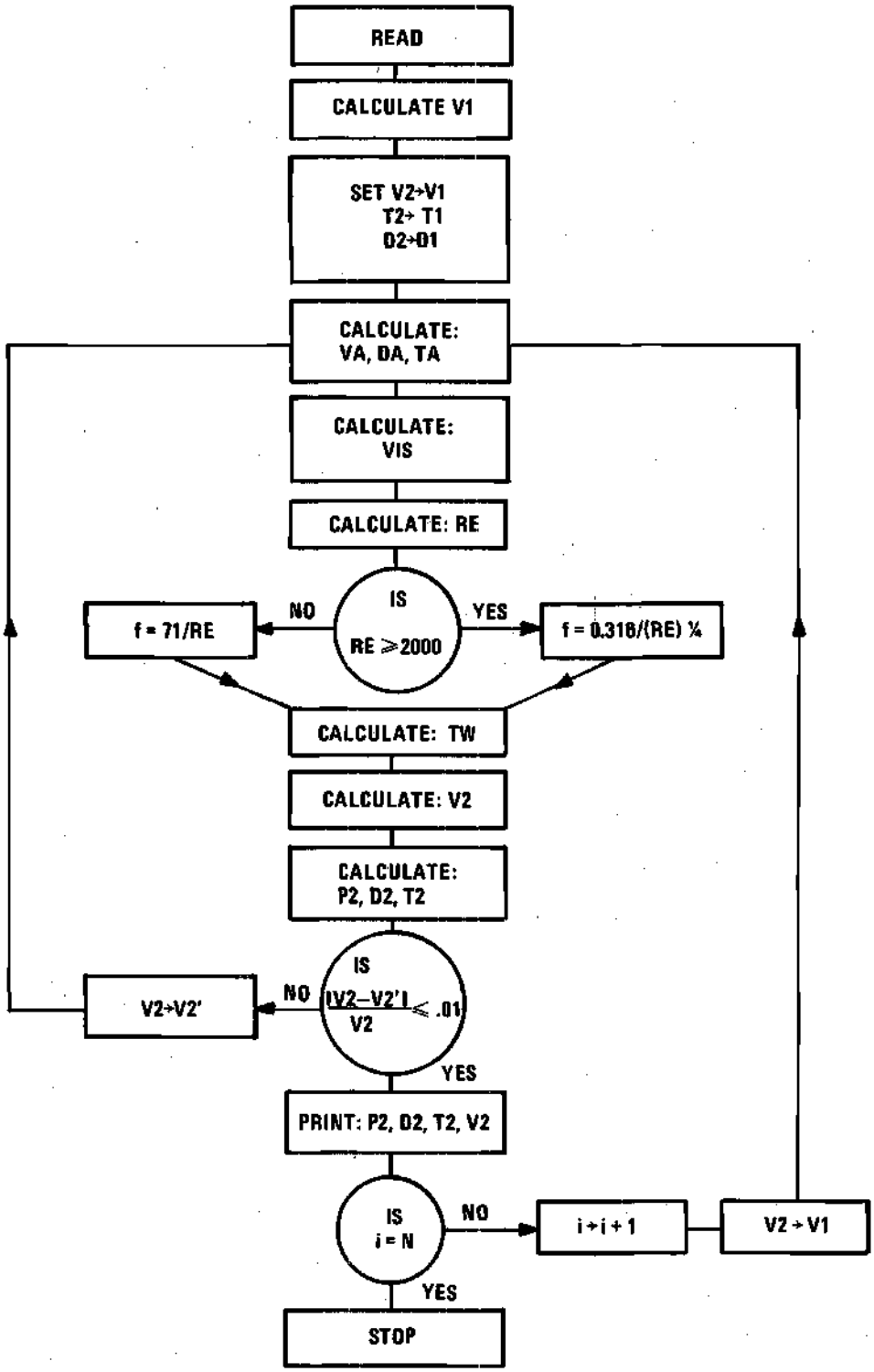

Table A-2. Computer Program

```
1.00  TYPE "COMPRESSOR ANALYSIS OF SINGLE WHEEL TURBINE"←
2.00  TYPE "SPECIFY PRESSURE IN LBF/FT2"←
2.01  READ P1←
2.02  TYPE "SPECIFY TEMPERATURE IN R"←
2.03  READ T1←
2.04  TYPE "SPECIFY DENSITY IN LBM/FT3"←
2.05  READ D1←
2.06  TYPE "SPECIFY MASS FLOW IN LBM/SEC"←
2.07  READ M←
2.08  TYPE "SPECIFY HEAT INPUT IN BTU/HR←
2.09  READ Q←
2.10  TYPE "SPECIFY WHEEL SPEED IN FT/SEC"←
2.11  READ U←
2.12  TYPE "SPECIFY WIDTH IN FT"←
2.13  READ W←
2.14  TYPE "SPECIFY HEIGHT IN FT"←
2.15  READ H←
2.16  TYPE "SPECIFY THE NUMBER OF SLOTS"←
2.17  READ R←
2.18  TYPE "SPECIFY INCREMENT Z IN FT"←
2.19  READ Z←
2.20  TYPE "SPECIFY THE NUMBER OF INCREMENTS"←
2.21  READ N←
3.00  SET V1 = M/(D1*H*W*R)←
3.01  SET V2 = V1←
3.02  SET T2 = T1←
3.03  SET D2 = D1←
3.04  SET I  = 1←
4.00  SET VA = (0.500)*(V1 + V2)←
4.01  SET TA = (0.500)*(T1 + T2)←
4.02  SET DA = (0.500)*(D1 + D2)←
4.03  SET VIS = (1.165E-5)*(EXP((0.71)*LN(TA/492)))←
```

Table A-2 (Continued)

```
4.04  SET RE = (DA*2*H*W*(U-VA))/(H+W)*(VIS))←
4.05  IF RE GEQ 2000 THEN GO TO 4.08←
4.06  SET F = (71)/(RE)←
4.07  GO TO 5.00←
4.08  SET F = 0.316/SQR(SQR(RE))
5.00  SET TW = (F*DA*(U-VA)*(U-VA))/(257.4)←
5.01  SET C1 = TW*((2*H+W)/(H*W))*Z+P1+(M*V1)/(H*W*R*32.17)←
5.02  SET C2 = (M)/(H*W*R*32.17)←
5.03  SET K1 = M/(64.4*R*H*W)-3.5*C2←
5.04  SET K2 = 3.5*C1←
5.05  SET K31 = Q/(4.63*H*W) + (TW*(2*H+W)*Z*U)/(H*W)←
5.06  SET K32 = 3.5*P1*V1+(M*V1+V1)/64.4*R*H*W)←
5.07  SET K3 = K31 + K32←
5.08  IF ABS((4*K1*K3)/(K2*K2)) GEQ 0.01 THEN GO TO 5.11←
5.09  SET V3 = K3/K2←
5.10  GO TO 5.12←
5.11  SET V3 = (-K2+SQR(K2*K2+4*K1*K3))/(2*K1)←
5.12  SET P2 = C1 - C2*V3←
5.13  SET D2 = M/(V3*R*H*W)←
5.14  SET T2 = P2/(53.3*D2)←
5.15  IF ABS((V3-V2)/V3) LEQ 1/(20*N) THEN GO TO 6.01←
5.16  SET V2 = V3←
5.17  GO TO 4.00←
6.01  FORM && IS I, &&&&&.&& IS P2, &&&&.& IS T2, &&&.&&&&& IS D2←
6.02  FORM @@@@@@@@@@ IS RE, @@@@@@@@@@ IS F, &&&&&.& IS V3←
6.03  PRINT FORM 6.01, I, P2, T2, D2←
6.04  PRINT FORM 6.02, RE, F, V3←
6.05  IF I EQL N THEN GO TO 6.12←
6.06  SET I = I+1←
6.07  SET V1 = V3←
6.08  SET T1 = T2←
6.09  SET P1 = P2←
6.10  SET D1 = D2←
```

Table A-2 (Continued)

```
6.11    GO TO 4.00←
6.12    STOP←
```

Table A-3. Typical Computer Readout

N = 42,000 RPM $f = 0.2/Re^{\frac{1}{4}}$

Q = 0 U = 1,200 W = 0.00521 H = 0.0359

R = 10 Z = 0.067 N = 10

P_1 = 2113 T_1 = 530 D_1 = 0.0753 M = 0.00628

```
1      IS I,  2235.43 IS P2,  762.3 IS T2,  0.05502 IS D2
4.818@+04 IS RE, 1.350@-02 IS F,   61.0 IS V3
2      IS I,  2339.30 IS P2,  963.7 IS T2,  0.04554 IS D2
2.986@+04 IS RE, 1.521@-02 IS F,   73.7 IS V3
3      IS I,  2432.92 IS P2, 1145.0 IS T2,  0.03986 IS D2
2.177@+04 IS RE, 1.647@-02 IS F,   84.2 IS V3
4      IS I,  2519.59 IS P2, 1312.7 IS T2,  0.03601 IS D2
1.714@+04 IS RE, 1.748@-02 IS F,   93.2 IS V3
5      IS I,  2601.27 IS P2, 1470.7 IS T2,  0.03318 IS D2
1.421@+04 IS RE, 1.832@-02 IS F,  101.2 IS V3
6      IS I,  2679.05 IS P2, 1621.0 IS T2,  0.03101 IS D2
1.216@+04 IS RE, 1.905@-02 IS F,  108.3 IS V3
7      IS I,  2753.69 IS P2, 1765.2 IS T2,  0.02927 IS D2
1.064@+04 IS RE, 1.969@-02 IS F,  114.7 IS V3
8      IS I,  2825.71 IS P2, 1904.2 IS T2,  0.02784 IS D2
9.474@+03 IS RE, 2.027@-02 IS F,  120.6 IS V3
9      IS I,  2895.53 IS P2, 2038.9 IS T2,  0.02664 IS D2
8.545@+03 IS RE, 2.080@-02 IS F,  126.0 IS V3
10     IS I,  2963.44 IS P2, 2169.9 IS T2,  0.02562 IS D2
7.789@+03 IS RE, 2.129@-02 IS F,  131.0 IS V3
STOP AT STATEMENT 6.12
:
```

Table A-3. (Continued)

P_1 = 2088 T_1 = 528 D_1 = 0.0746 M = 0.01885

```
1      IS I,  2197.87 IS P2,  597.2 IS T2,  0.06905 IS D2
5.392@+04 IS RE, 1.312@-02 IS F,  145.9 IS V3
2      IS I,  2302.85 IS P2,  665.8 IS T2,  0.06489 IS D2
4.591@+04 IS RE, 1.366@-02 IS F,  155.3 IS V3
3      IS I,  2404.02 IS P2,  731.8 IS T2,  0.06163 IS D2
4.004@+04 IS RE, 1.414@-02 IS F,  163.5 IS V3
4      IS I,  2502.11 IS P2,  795.7 IS T2,  0.05900 IS D2
3.558@+04 IS RE, 1.456@-02 IS F,  170.8 IS V3
5      IS I,  2597.64 IS P2,  857.8 IS T2,  0.05682 IS D2
3.208@+04 IS RE, 1.494@-02 IS F,  177.4 IS V3
6      IS I,  2691.00 IS P2,  918.4 IS T2,  0.05498 IS D2
2.926@+04 IS RE, 1.529@-02 IS F,  183.3 IS V3
7      IS I,  2782.50 IS P2,  977.7 IS T2,  0.05340 IS D2
2.693@+04 IS RE, 1.561@-02 IS F,  188.7 IS V3
8      IS I,  2872.38 IS P2, 1035.9 IS T2,  0.05202 IS D2
2.497@+04 IS RE, 1.591@-02 IS F,  193.7 IS V3
9      IS I,  2960.85 IS P2, 1093.1 IS T2,  0.05082 IS D2
2.331@+04 IS RE, 1.619@-02 IS F,  198.3 IS V3
10     IS I,  3048.06 IS P2, 1149.5 IS T2,  0.04975 IS D2
2.187@+04 IS RE, 1.645@-02 IS F,  202.6 IS V3
STOP AT STATEMENT 6.12
:
```

Table A-3. (Continued)

P_1 = 2033 T_1 = 524 D_1 = 0.0733 M = 0.03143

```
1      IS I,  2126.92 IS P2,  557.2 IS T2,  0.07162 IS D2
5.123@+04 IS RE, 1.329@-02 IS F,  234.6 IS V3
2      IS I,  2219.73 IS P2,  593.5 IS T2,  0.07017 IS D2
4.771@+04 IS RE, 1.353@-02 IS F,  239.5 IS V3
3      IS I,  2311.63 IS P2,  629.4 IS T2,  0.06891 IS D2
4.460@+04 IS RE, 1.376@-02 IS F,  243.9 IS V3
4      IS I,  2402.76 IS P2,  664.9 IS T2,  0.06780 IS D2
4.193@+04 IS RE, 1.398@-02 IS F,  247.8 IS V3
5      IS I,  2493.21 IS P2,  700.1 IS T2,  0.06682 IS D2
3.960@+04 IS RE, 1.418@-02 IS F,  251.5 IS V3
6      IS I,  2583.08 IS P2,  735.0 IS T2,  0.06593 IS D2
3.755@+04 IS RE, 1.437@-02 IS F,  254.9 IS V3
7      IS I,  2672.43 IS P2,  769.7 IS T2,  0.06514 IS D2
3.572@+04 IS RE, 1.455@-02 IS F,  258.0 IS V3
8      IS I,  2761.33 IS P2,  804.2 IS T2,  0.06442 IS D2
3.409@+04 IS RE, 1.472@-02 IS F,  260.8 IS V3
9      IS I,  2849.83 IS P2,  838.5 IS T2,  0.06377 IS D2
3.263@+04 IS RE, 1.488@-02 IS F,  263.5 IS V3
10     IS I,  2937.98 IS P2,  872.6 IS T2,  0.06317 IS D2
3.130@+04 IS RE, 1.504@-02 IS F,  266.0 IS V3
STØP AT STATEMENT 6.12
:
```

Table A-3. (Continued)

P_1 = 1954 T_1 = 518 D_1 = 0.0712 M = 0.04398

```
1      IS I,  2032.17 IS P2,  536.4 IS T2,  0.07109 IS D2
4.663@+04 IS RE, 1.361@-02 IS F,  330.8 IS V3
2      IS I,  2110.72 IS P2,  557.9 IS T2,  0.07098 IS D2
4.541@+04 IS RE, 1.370@-02 IS F,  331.3 IS V3
3      IS I,  2189.73 IS P2,  579.6 IS T2,  0.07088 IS D2
4.408@+04 IS RE, 1.380@-02 IS F,  331.7 IS V3
4      IS I,  2269.25 IS P2,  601.4 IS T2,  0.07079 IS D2
4.219@+04 IS RE, 1.395@-02 IS F,  332.2 IS V3
5      IS I,  2348.98 IS P2,  623.3 IS T2,  0.07071 IS D2
4.161@+04 IS RE, 1.400@-02 IS F,  332.5 IS V3
6      IS I,  2429.13 IS P2,  645.3 IS T2,  0.07063 IS D2
4.051@+04 IS RE, 1.410@-02 IS F,  332.9 IS V3
7      IS I,  2509.70 IS P2,  667.3 IS T2,  0.07056 IS D2
3.947@+04 IS RE, 1.419@-02 IS F,  333.3 IS V3
8      IS I,  2590.68 IS P2,  689.5 IS T2,  0.07049 IS D2
3.949@+04 IS RE, 1.428@-02 IS F,  333.6 IS V3
9      IS I,  2672.12 IS P2,  711.9 IS T2,  0.07042 IS D2
3.709@+04 IS RE, 1.441@-02 IS F,  333.9 IS V3
10     IS I,  2753.75 IS P2,  734.2 IS T2,  0.07036 IS D2
3.665@+04 IS RE, 1.445@-02 IS F,  334.2 IS V3
STØP AT STATEMENT 6.12
:
```

Table A-3. (Continued)

P_1 = 1808 T_1 = 506 D_1 = 0.0674 M = 0.5655

```
1      IS I,  1870.41 IS P2,  516.1 IS T2,  0.06800 IS D2
3.878@+04 IS RE, 1.425@-02 IS F,  444.6 IS V3
2      IS I,  1933.74 IS P2,  529.1 IS T2,  0.06857 IS D2
3.870@+04 IS RE, 1.426@-02 IS F,  440.9 IS V3
3      IS I,  1998.02 IS P2,  542.3 IS T2,  0.06913 IS D2
3.852@+04 IS RE, 1.428@-02 IS F,  437.4 IS V3
4      IS I,  2063.23 IS P2,  555.7 IS T2,  0.06965 IS D2
3.832@+04 IS RE, 1.429@-02 IS F,  434.1 IS V3
5      IS I,  2129.35 IS P2,  569.4 IS T2,  0.07016 IS D2
3.810@+04 IS RE, 1.431@-02 IS F,  430.9 IS V3
6      IS I,  2196.36 IS P2,  583.3 IS T2,  0.07065 IS D2
3.787@+04 IS RE, 1.434@-02 IS F,  428.0 IS V3
7      IS I,  2264.25 IS P2,  597.4 IS T2,  0.07111 IS D2
3.762@+04 IS RE, 1.436@-02 IS F,  425.2 IS V3
8      IS I,  2333.01 IS P2,  611.7 IS T2,  0.07156 IS D2
3.737@+04 IS RE, 1.439@-02 IS F,  422.5 IS V3
9      IS I,  2402.62 IS P2,  626.1 IS T2,  0.07199 IS D2
3.710@+04 IS RE, 1.441@-02 IS F,  420.0 IS V3
10     IS I,  2473.05 IS P2,  640.8 IS T2,  0.07241 IS D2
3.682@+04 IS RE, 1.444@-02 IS F,  417.6 IS V3
STØP AT STATEMENT 6.12
:
```

Table A-3. (Continued)

P_1 = 1611 T_1 = 490 D_1 = 0.0621 M = 0.06912

```
1      IS I,  1658.23 IS P2,  494.1 IS T2,  0.06296 IS D2
2.974@+04 IS RE, 1.523@-02 IS F,  586.9 IS V3
2      IS I,  1706.40 IS P2,  501.7 IS T2,  0.06381 IS D2
3.029@+04 IS RE, 1.516@-02 IS F,  579.1 IS V3
3      IS I,  1755.57 IS P2,  509.5 IS T2,  0.06465 IS D2
3.074@+04 IS RE, 1.510@-02 IS F,  571.6 IS V3
4      IS I,  1805.73 IS P2,  517.4 IS T2,  0.06547 IS D2
3.115@+04 IS RE, 1.505@-02 IS F,  564.4 IS V3
5      IS I,  1856.89 IS P2,  525.6 IS T2,  0.06628 IS D2
3.154@+04 IS RE, 1.501@-02 IS F,  557.5 IS V3
6      IS I,  1909.05 IS P2,  534.0 IS T2,  0.06708 IS D2
3.191@+04 IS RE, 1.496@-02 IS F,  550.9 IS V3
7      IS I,  1962.22 IS P2,  542.5 IS T2,  0.06786 IS D2
3.224@+04 IS RE, 1.493@-02 IS F,  544.6 IS V3
8      IS I,  2016.39 IS P2,  551.3 IS T2,  0.06862 IS D2
3.255@+04 IS RE, 1.489@-02 IS F,  538.5 IS V3
9      IS I,  2071.57 IS P2,  560.3 IS T2,  0.06937 IS D2
3.283@+04 IS RE, 1.486@-02 IS F,  532.7 IS V3
10     IS I,  2127.75 IS P2,  569.4 IS T2,  0.07011 IS D2
3.309@+04 IS RE, 1.483@-02 IS F,  527.1 IS V3
STØP AT STATEMENT 6.12
:
```

Table B-1. Titanium Wheel With Graphite Seals-Room Temperature 77°F-Line Pressure 80 psig.

N	LAMINAR ELEMENT AT COMPRESSOR OUTLET		P	T_1	T_3	T_2	T_C	Q
RPM	IN. OIL	IN. WATER	IN. HG	°F	°F	°F	°F	SCFM
15,000	3.3	2.75	0.4	116	128	122	0.85	30.94
"	2.1	1.75	1.2	116	128	122	0.85	19.89
"	0.9	0.75	2.4	136	142	131	0.83	8.3
"	0	0	3.2	146	154	112	0.88	0
24,000	5.3	4.42	0.4	124	142	133	0.82	47.5
"	4.0	3.34	2.4	136	159	153	0.77	33.8
"	2.7	2.25	4.0	151	170	167	0.74	22
"	0	0	7.2	212	227	128	0.84	0
30,000	6.9	5.75	0.6	154	184	176	0.72	54
"	4.9	4.09	3.8	164	198	195	0.68	36.6
"	2.5	2.05	7.0	196	269	258	0.56	15.2
"	0	0	10.0	309	339	183	0.7	0
42,000	9.5	7.92	0.9	207	278	278	0.53	54.5
"	7.4	6.17	5.4	318	362	316	0.465	37.2
"	2.2	7.67	13.2	326	399	340	0.43	12.5
"	0	0	15.4	432	482	259	0.55	0

Table B-2. Titanium Wheel with Graphite Seals (After Running, Seals were Badly Damaged) Room Temperature 71°F-Line Pressure 80 psig.

N	LAMINAR ELEMENT AT COMPRESSOR OUTLET		P	T_1	T_3	T_2	T_C	Q
RPM	IN. OIL	IN. WATER	IN. HG	°F	°F	°F	°F	SCFM
30,000	4.9	4.09	0.5	116	146	146	0.79	42.7
"	4.5	3.75	2.0	131	167	167	0.74	36.6
"	3.6	3.00	3.4	146	185	179	0.71	28.1
"	2.6	2.17	4.8	167	206	197	0.67	19.2
"	0	0	7.6	221	266	155	-	0

Table B-3. Titanium Wheel with Graphite Seals (Some Tips on Seal were Broken) Room Temperature 71°F.-Line Pressure 80 psig.

N	LAMINAR ELEMENT AT COMPRESSOR OUTLET		P	T_1	T_3	T_2	T_C	Q
RPM	IN. OIL	IN. WATER	IN. HG	°F	°F	°F	°F	SCFM
15,000	2.9	2.42	0.35	113	133	130	0.85	27.4
"	1.3	1.08	1.8	141	160	154	0.77	11.1
"	0.4	0.33	2.6	212	230	224	0.62	2.68
24,000	4.5	3.76	0.6	117	146	143	0.79	39.5
"	2.1	1.75	4.0	162	193	185	0.7	16.3
"	0.7	0.58	5.5	237	264	248	0.58	4.5
30,000	5.7	4.75	0.8	135	179	179	0.71	44.3
"	3.5	2.82	5.1	185	244	244	0.58	21.6
"	0.4	3.34	8.2	256	308	207	0.65	2.8

Table B-4. Titanium Wheel With Graphite Seals (Readjust Seals of Table 3) Room Temperature 71°F. Line Pressure 80 psig.

N	LAMINAR ELEMENT AT COMPRESSOR OUTLET		P	T_1	T_3	T_2	T_C	Q
RPM	IN. OIL	IN. WATER	IN. HG	°F	°F	°F	°F	SCFM
30,000	5.6	4.66	2.0	144	182	177	0.71	43.8
"	3.7	3.08	5.0	169	222	214	0.64	26.0
"	2.1	1.75	6.7	202	262	243	0.58	13.6
"	0	0	9.4	-	-	-	-	0

TABLE C–1 FLOW RATE CORRECTION FACTOR VERSUS TEMPERATURE

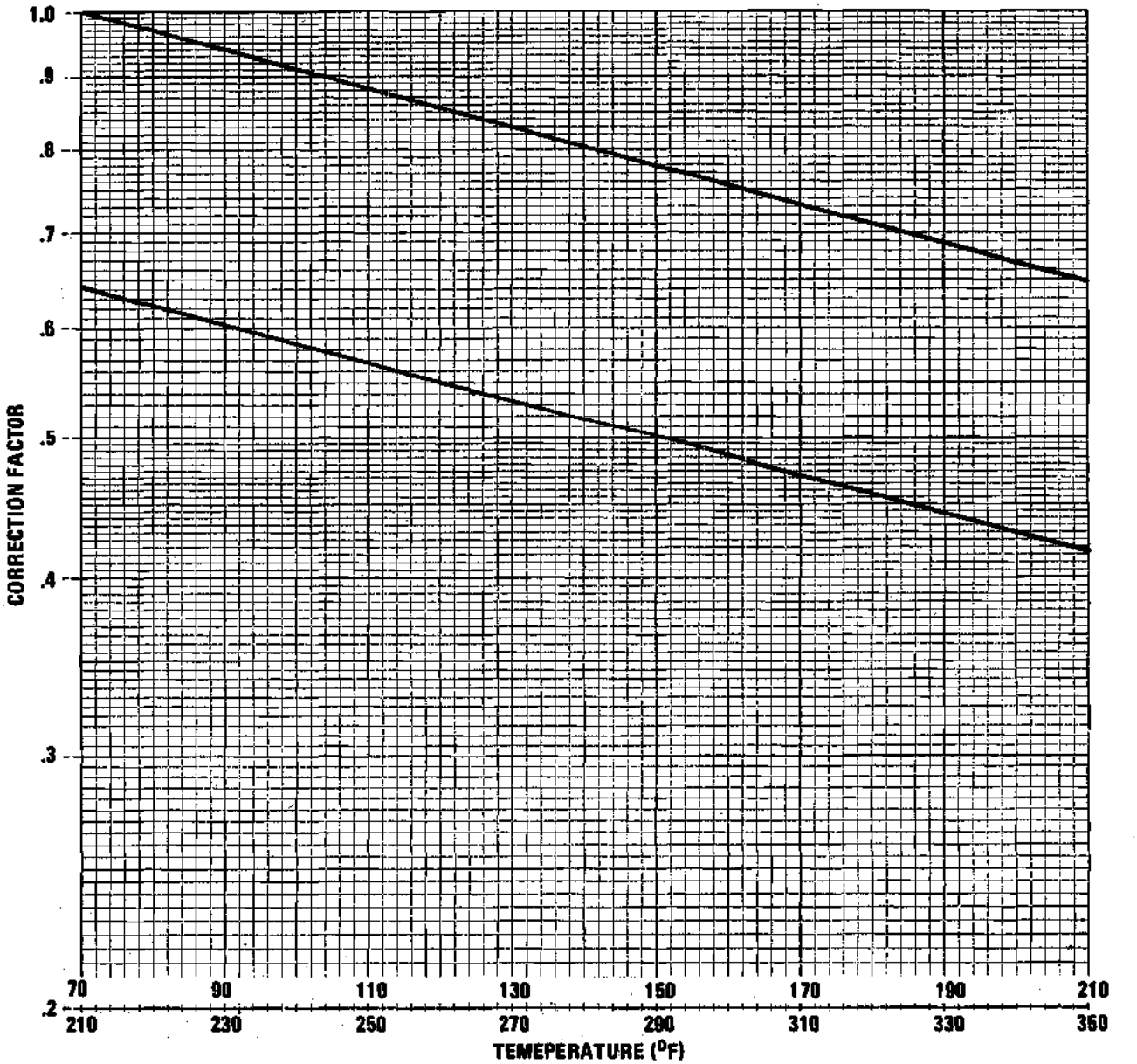

TABLE C-2. CALIBRATION CURVE MERIAM LAMINAR FLOW ELEMENT MODEL 50 MC 2-2P SERIAL NO. B-40841

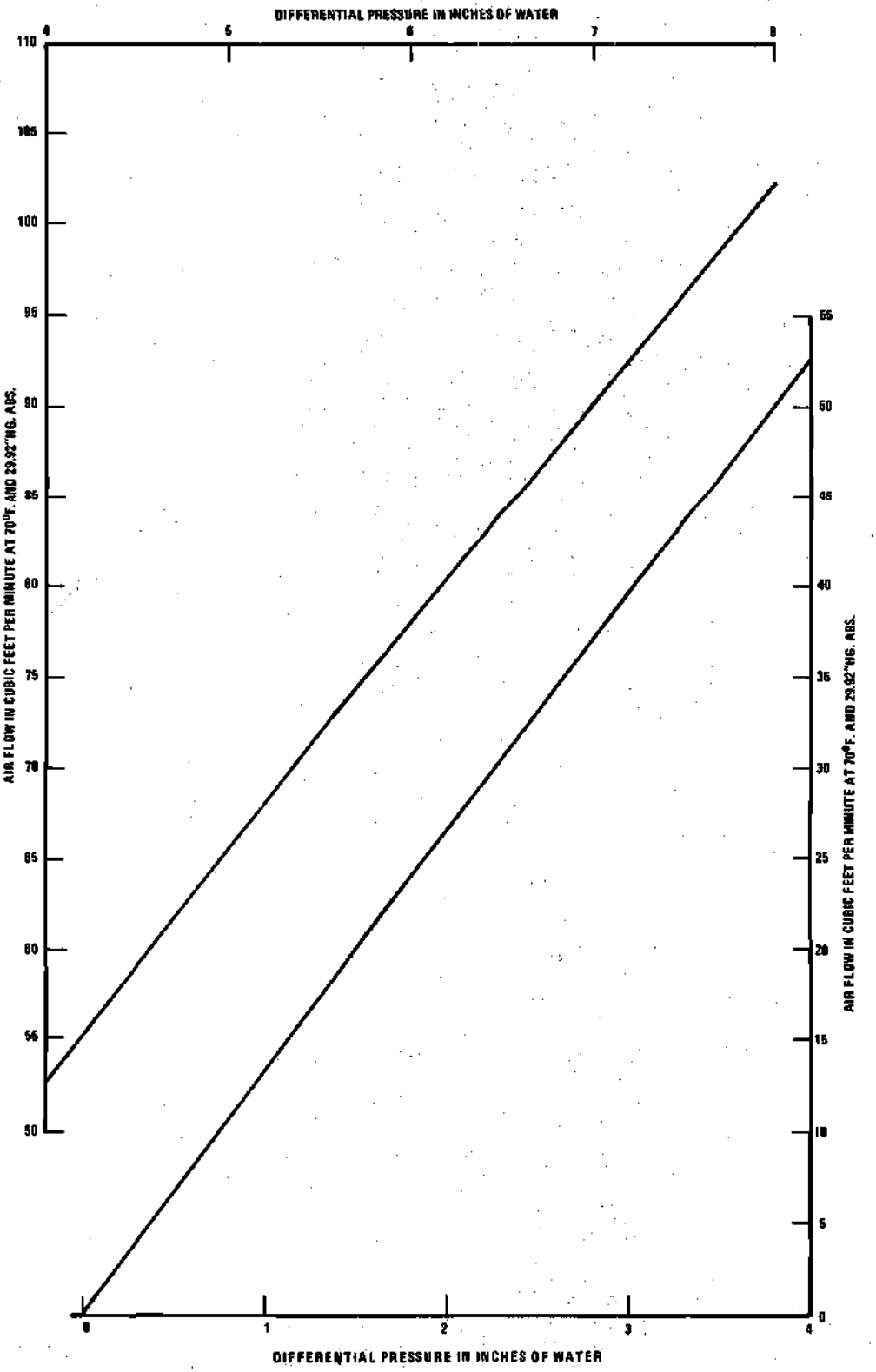

REFERENCES

1. A. H. Shapiro, Compressible Fluid Flow, (New York: The Ronadl Press Company, 1953), Volume I, pp. 184-186, pp. 82-83.

2. H. Schlicting, Boundary Layer Theory, (New York: McGraw-Hill Book Company, Inc., 1968), 6th Edition, pp. 560-575, pp. 575-578.

3. Burgess H. Jennings and Willard L. Rogers, Gas Turbine Analysis and Practice, (New York: McGraw-Hill Book Company, Inc., 1953).

4. J. H. Keenan and J. Kaye, Gas Tables (New York: John Wiley and Sons, Inc., 1948), pp. 392-402.

5. V. M. Faires, Elementary Thermodynamics, (New York: The Macmillan Company, 1957), 3th Edition, pp. 135-136.

6. S. Timoshenko, Strength of Materials (New York: D. Van Norstrand Company, Inc., 1956) pp. 223-228.

7. L. A. Dorfman, Hydrodynamic Resistance and the Heat Loss of Rotating Solids (Oliver & Boyd, Ltd., 1963) pp. 55-76.

8. K. E. Boyd and W. Rice, "Laminar Inward Flow of an Incompressible Fluid Between Rotating Disks with Peripheral Admission", Journal of Applied Mechanics, June 1968, pp. 229-237.

9. R. A. Conover, "Laminar Flow Between a Rotating Disk and a Parallel Stationary Wall with and without Radial Inflow", Journal of Basic Engineering, Sept. 1968, pp. 325-332.

10. D. P. Traviss, Georgia Institute of Technology Special Problem (September, 1969) under the supervision of Dr. G. T. Colwell, School of Mechanical Engineering.